GRAVITATIONAL WAVE DETECTION BY MICROWAVE RESONANT CAVITY

Danho Ahn (IBS-CAPP)

Center for Axion and Precision Physics Research, Institute of Basic Science,
Daejeon 34051, Republic of Korea

apctp asia pacific center for theoretical physics

KASI 한국천문연구원

Introduction:

Gravitational Wave

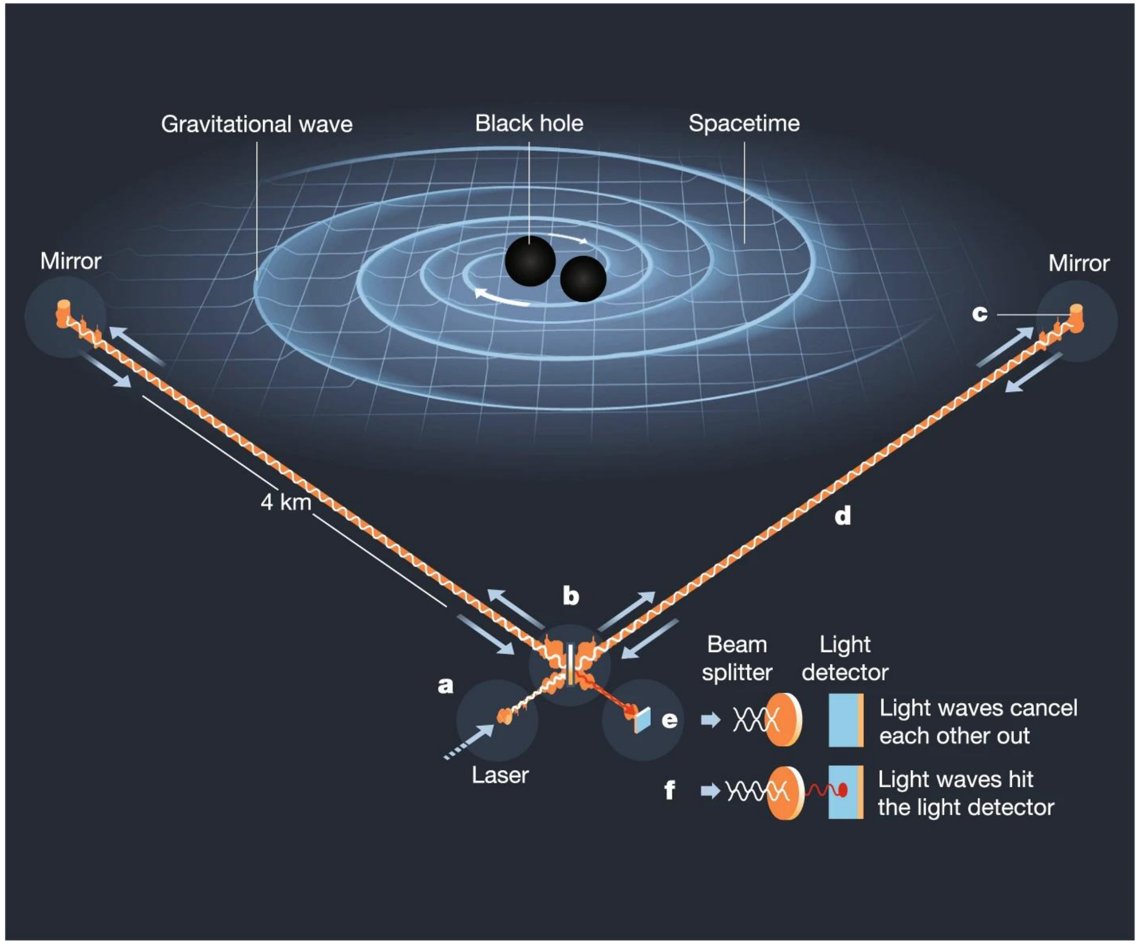

Miller, M.C., Yunes, N. Nature 568, 469–476 (2019).

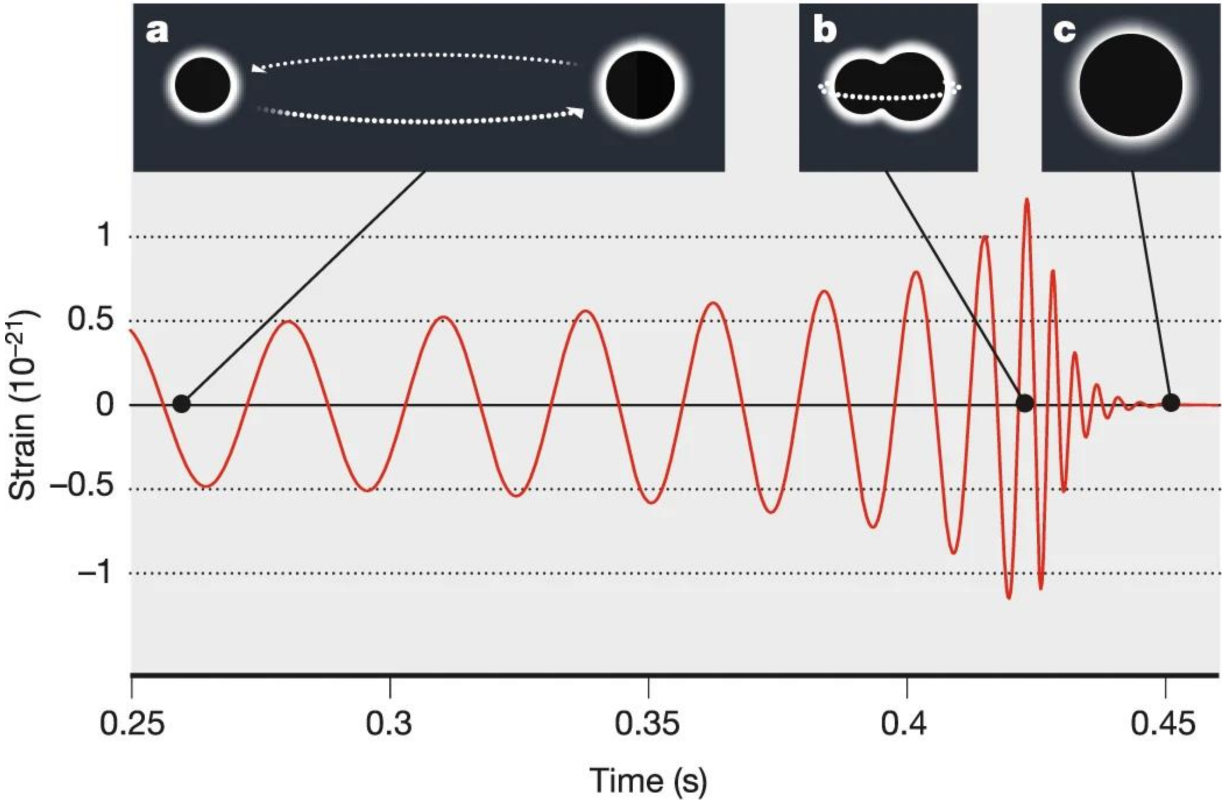

Introduction:

Gravitational Wave Search

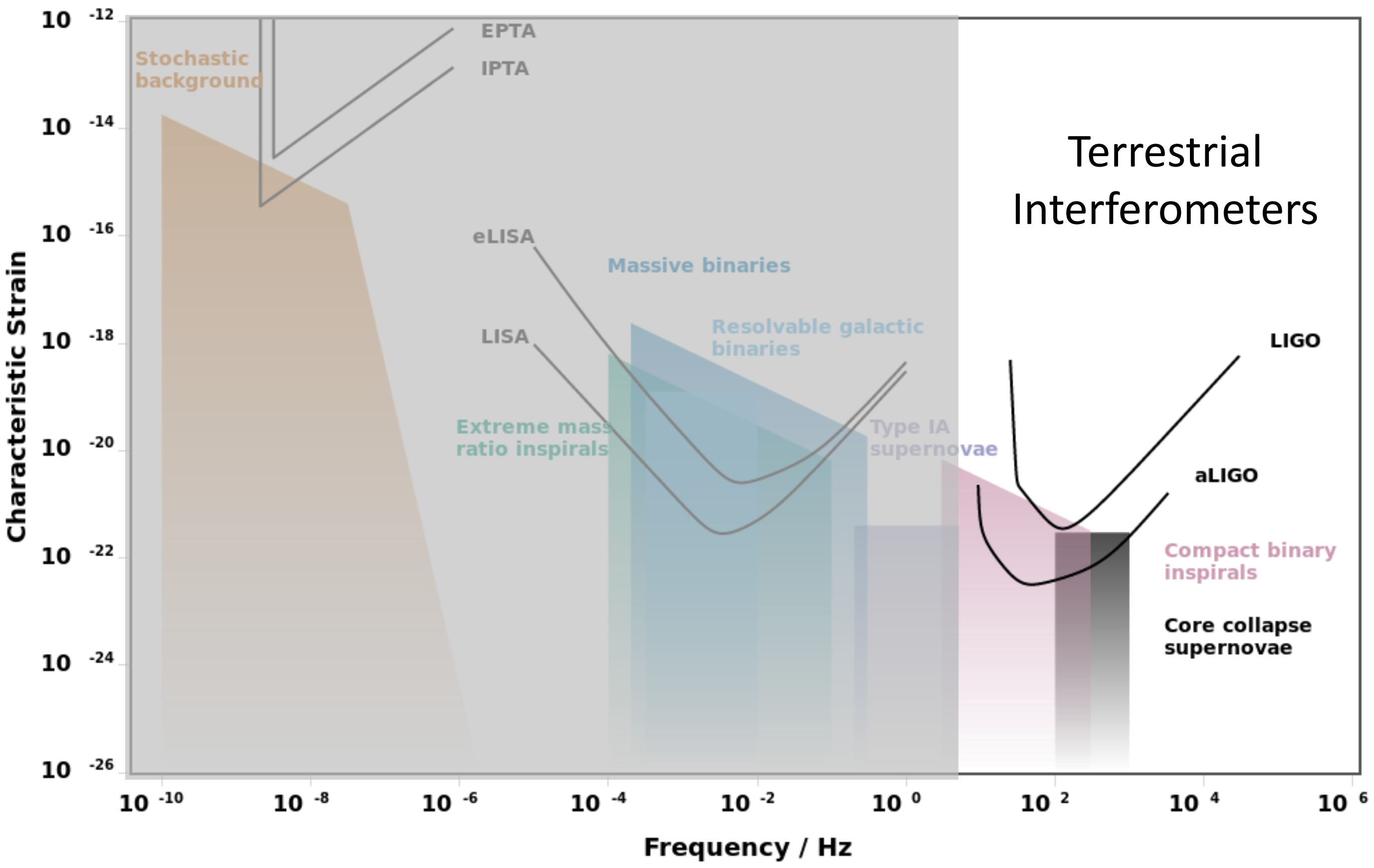

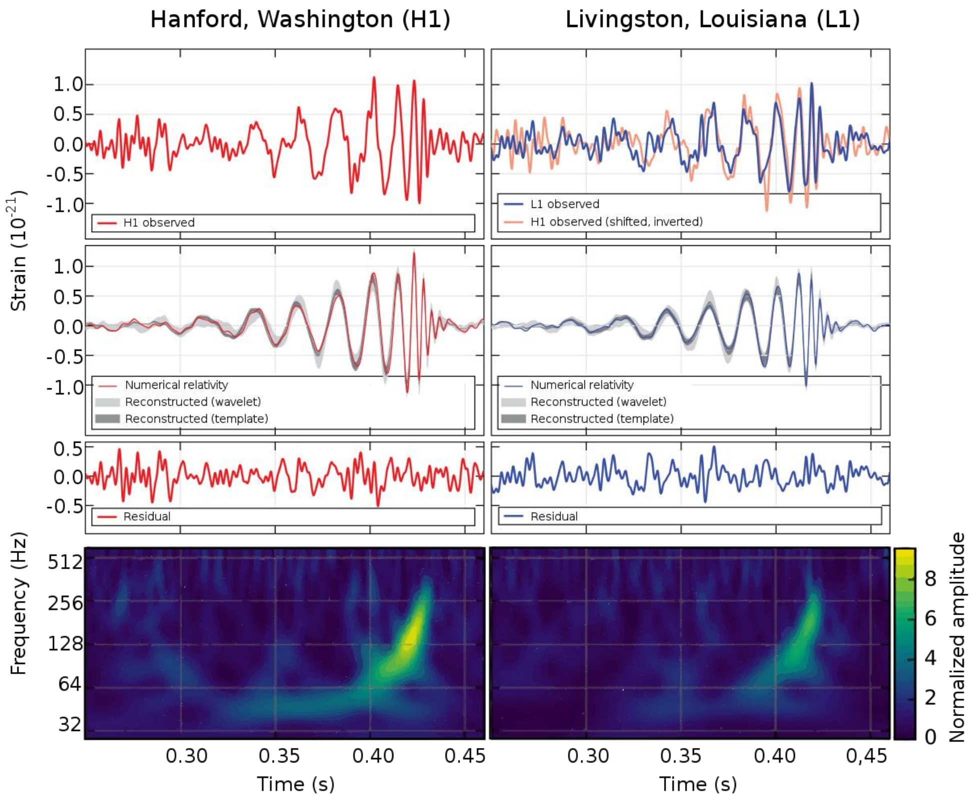

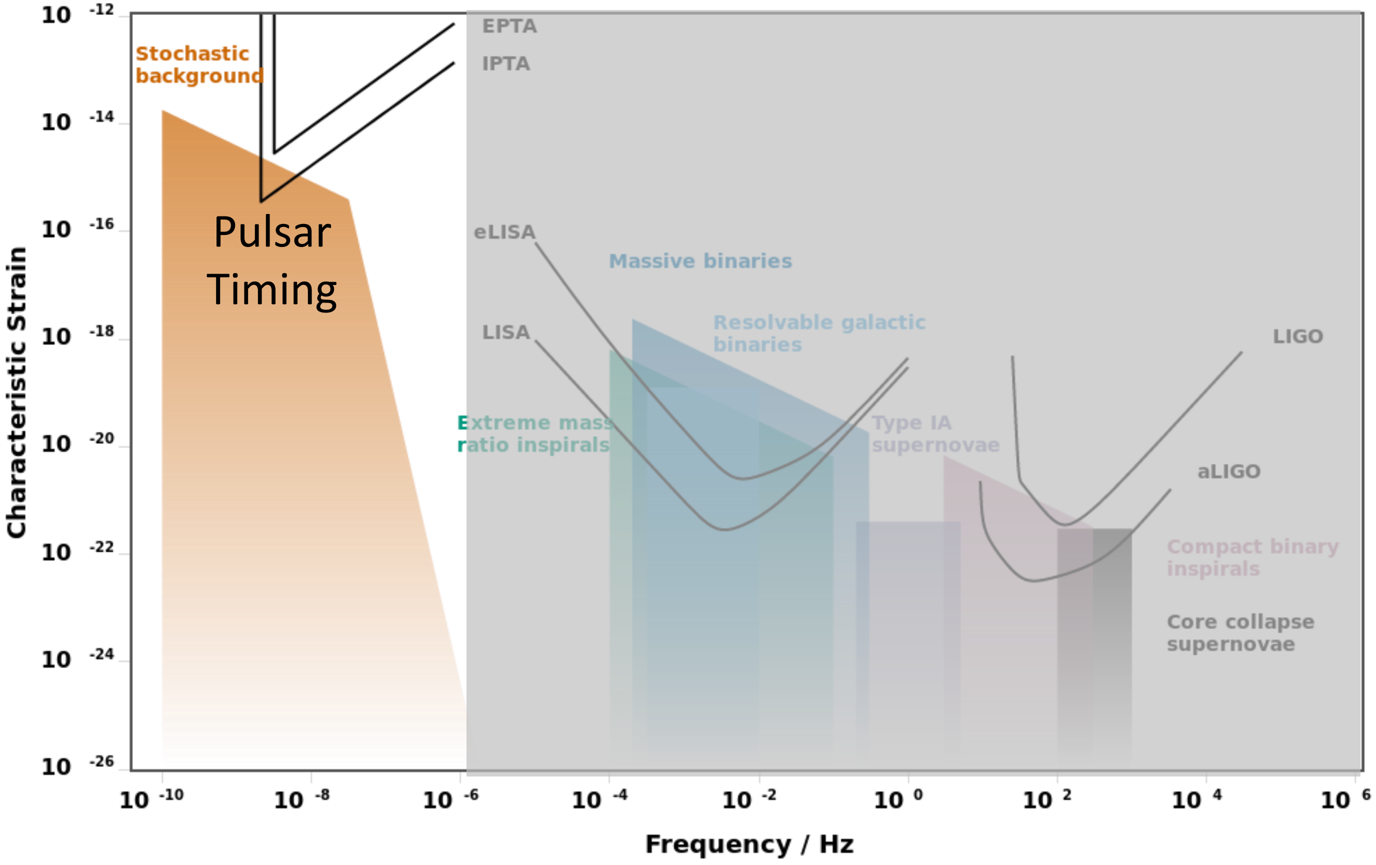

Hellings-Downs Curve

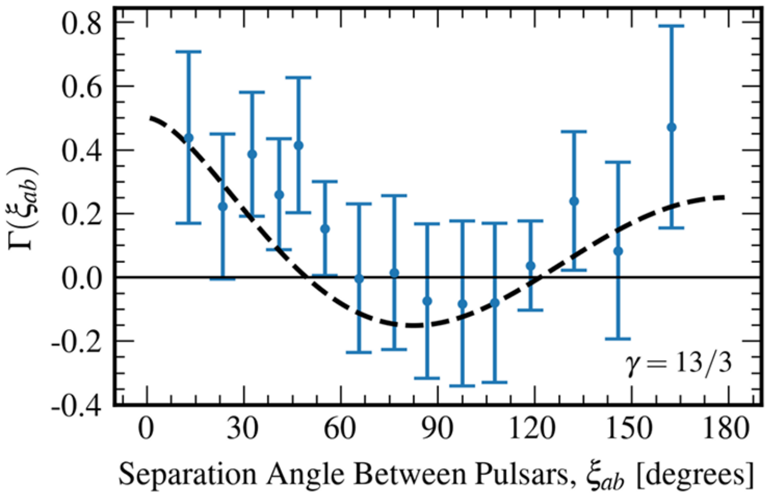

Astrophys.J.Lett. 956 (2023) 1, L3

Introduction:

Gravitational Wave Search

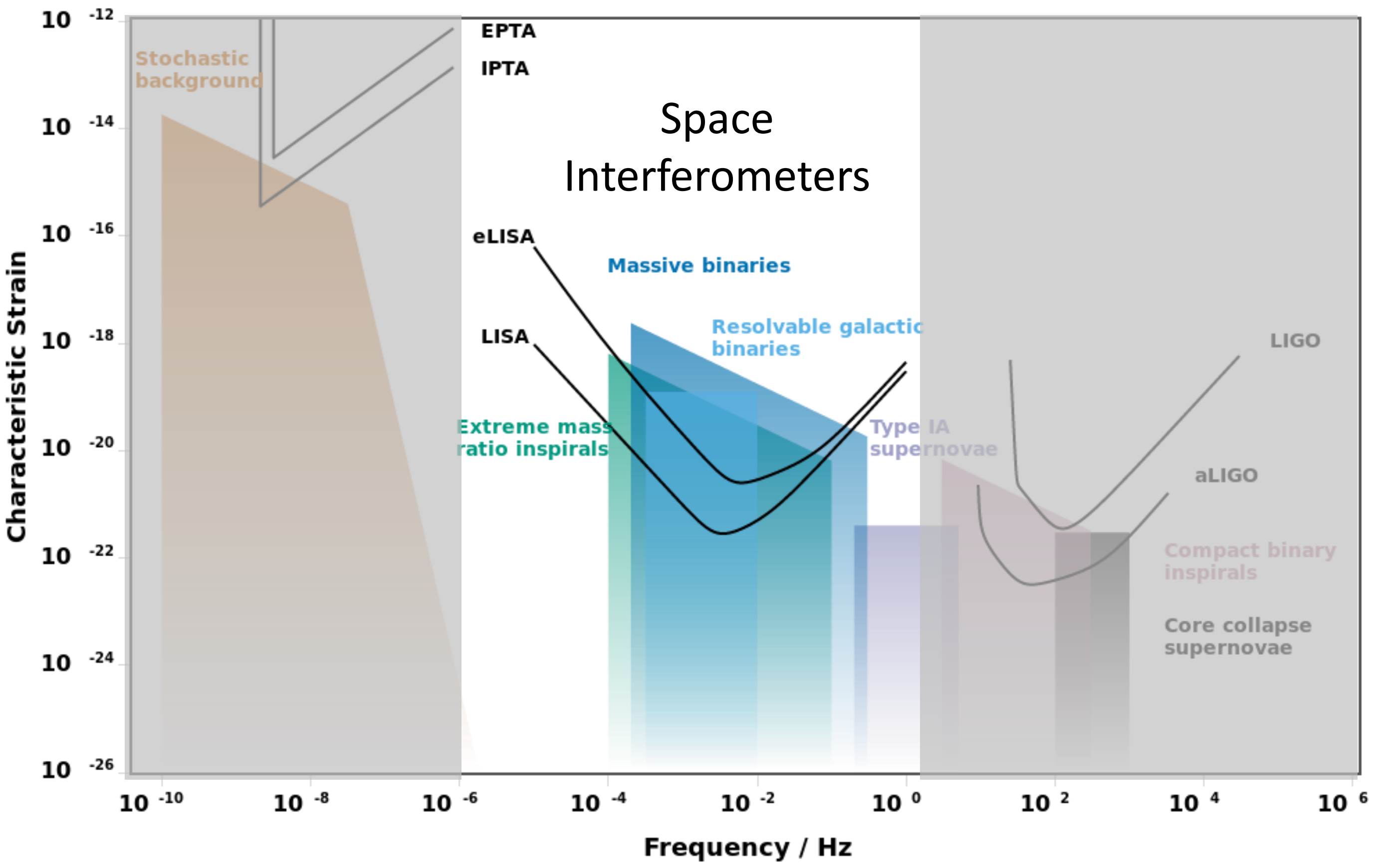

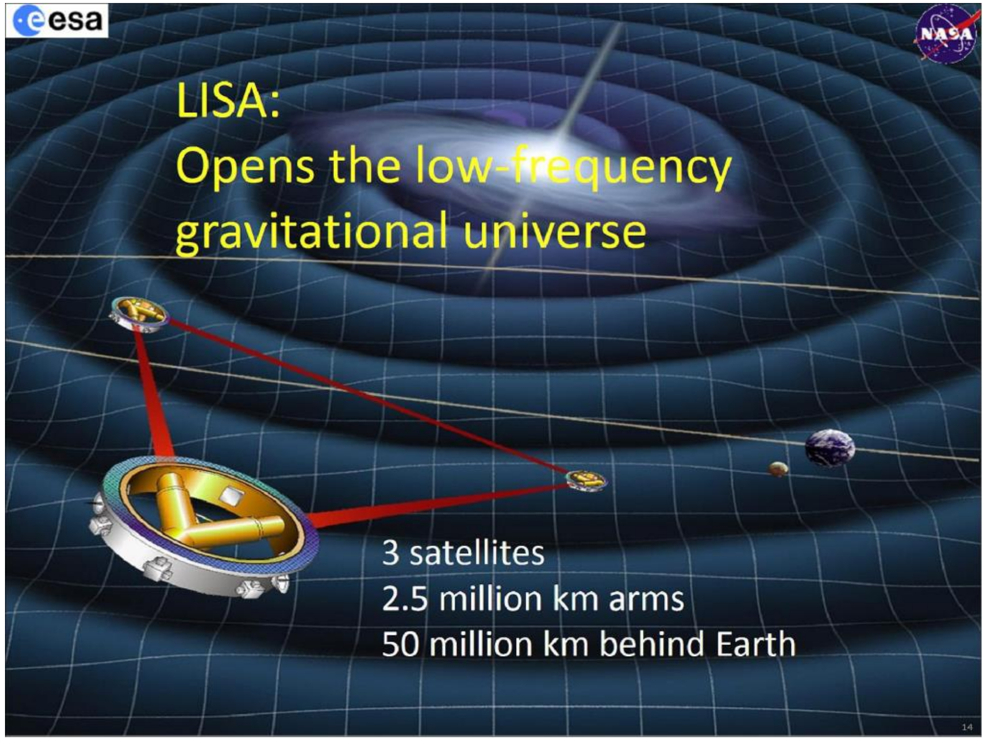

Introduction:

Gravitational Wave Search

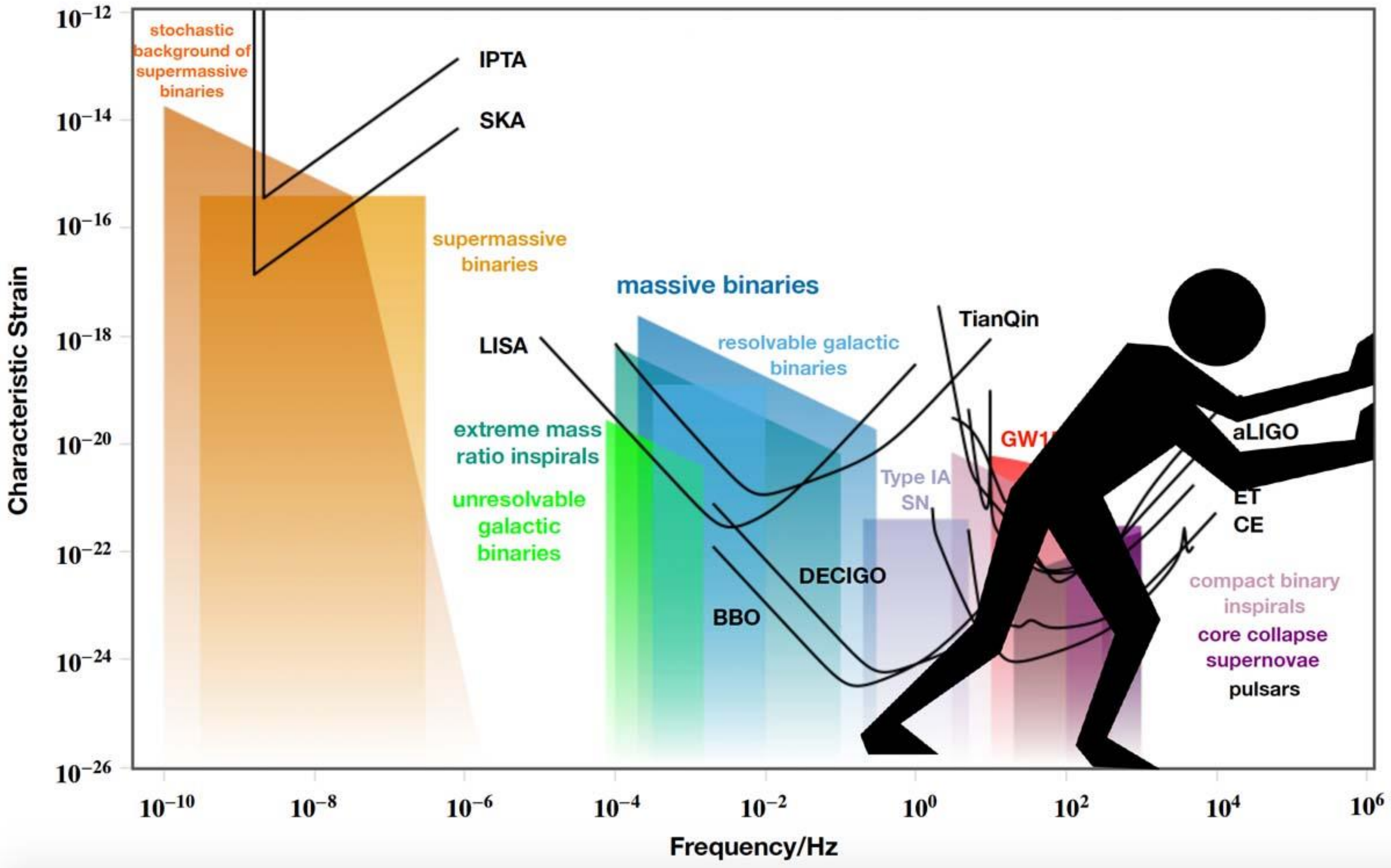

Introduction:

High Frequency Gravitational Wave Sources

Coherent

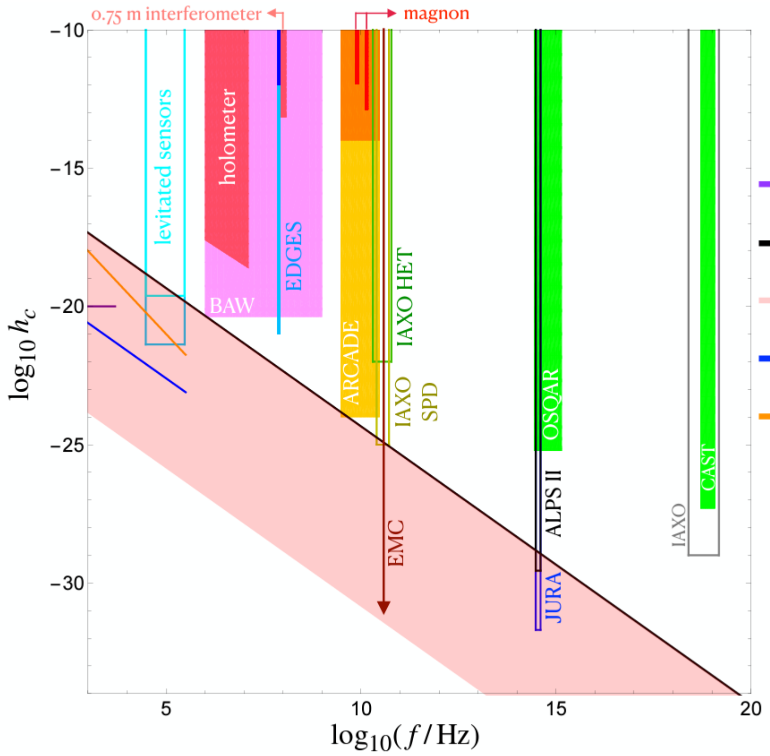

SOURCES LEGEND

- Neutron stars
- Primordial BHs
- Exotic compact objects
- Superradiance (annihilation)
- Superradiance (decay)

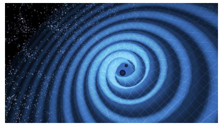

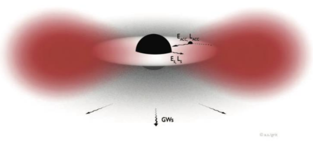

Stochastic

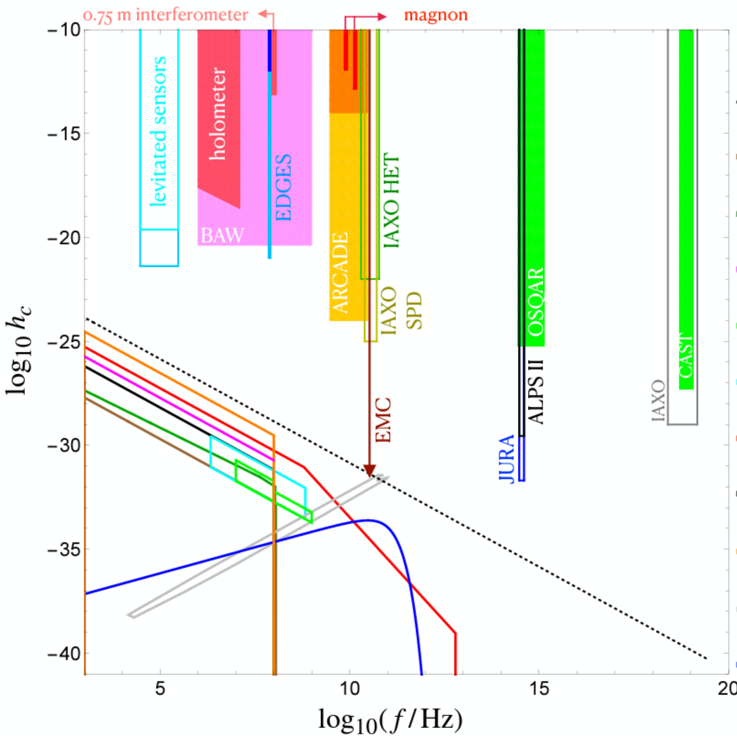

Living. Rev. Relativ. 24, 4 (2021).

Introduction:

Ultra High Frequency Gravitational Wave Sources

Coherent (Transient)

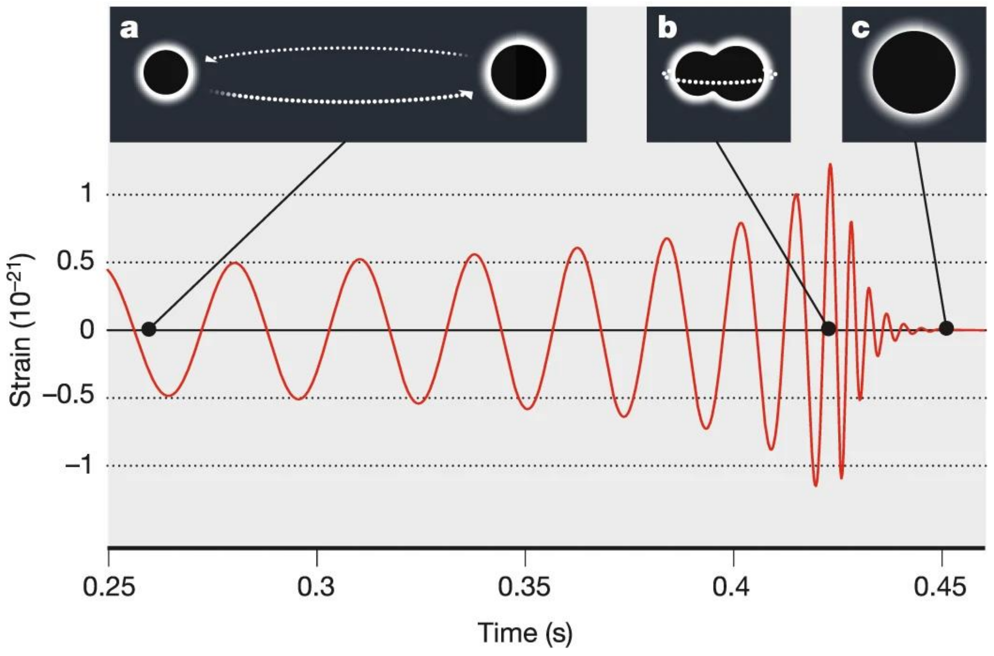

Miller, M.C., Yunes, N. Nature 568, 469–476 (2019).

Stochastic

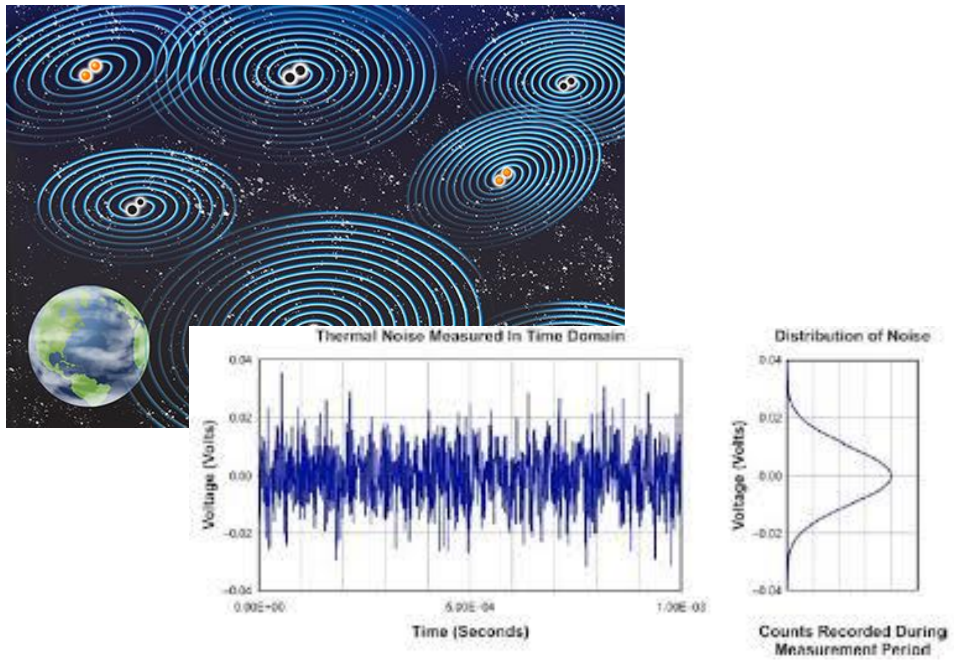

https://physics.aps.org/articles/v13/113

Introduction:

Ultra High Frequency Gravitational Wave Sources

Coherent (Monochromatic)

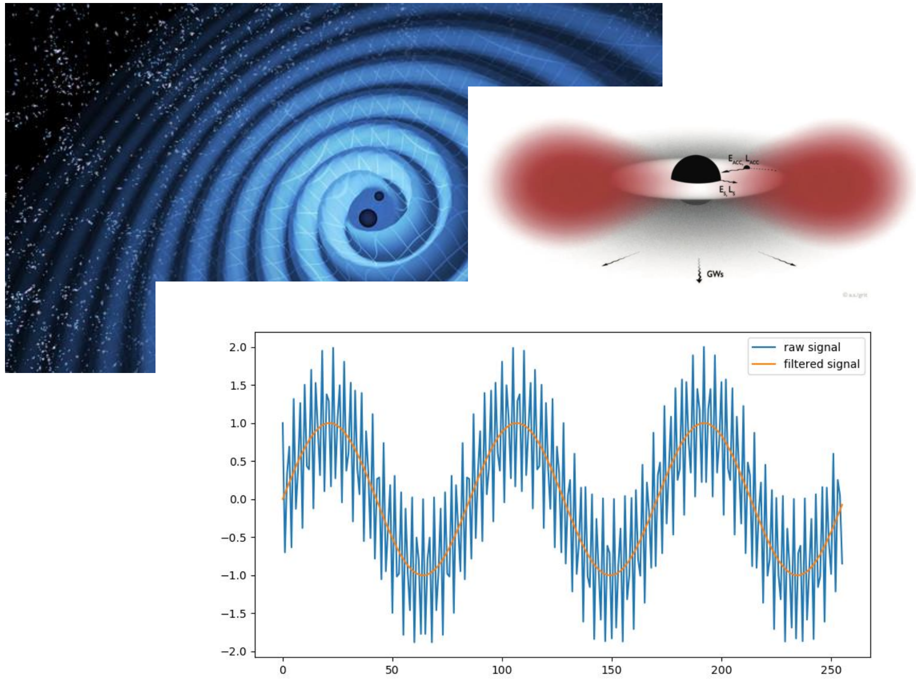

Stochastic

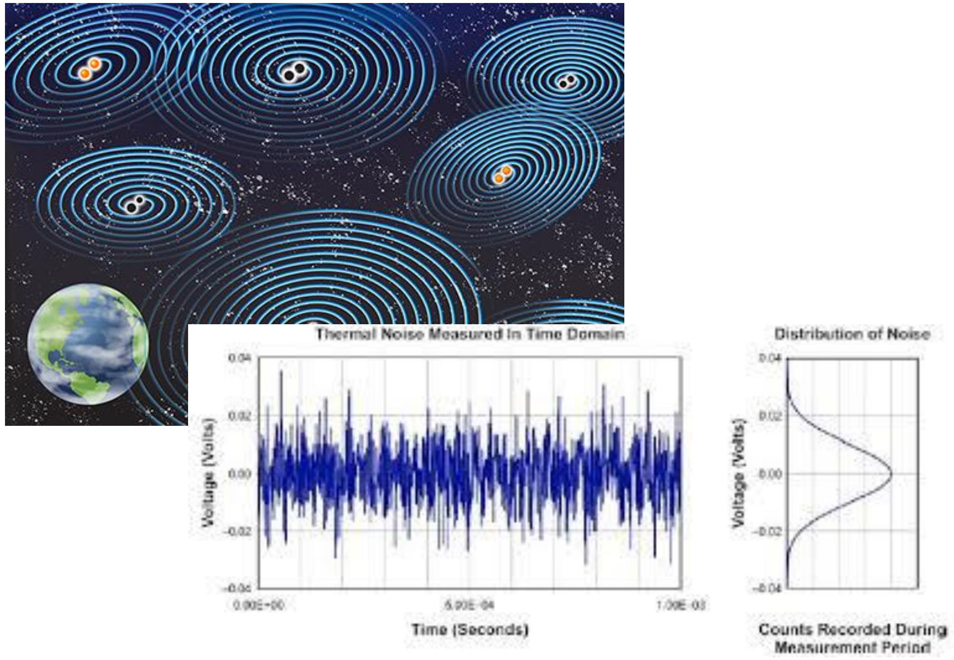

https://physics.aps.org/articles/v13/113

Introduction:

Ultra High Frequency Gravitational Wave Sources

Coherent (Monochromatic)

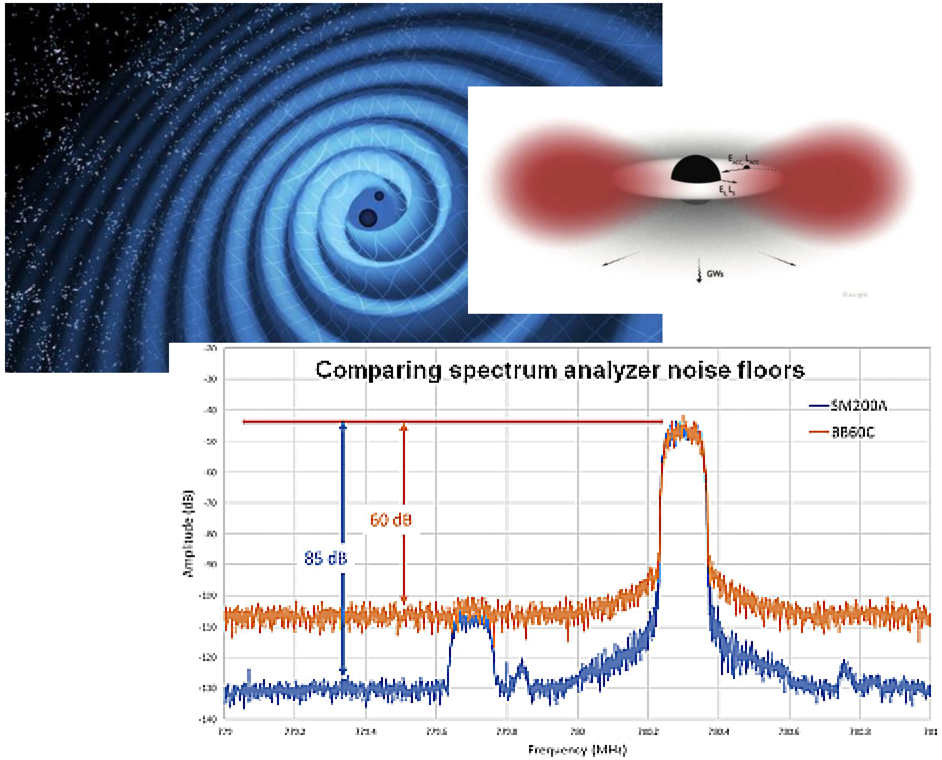

Axion Signal

Turner, PRD 42 (1990).

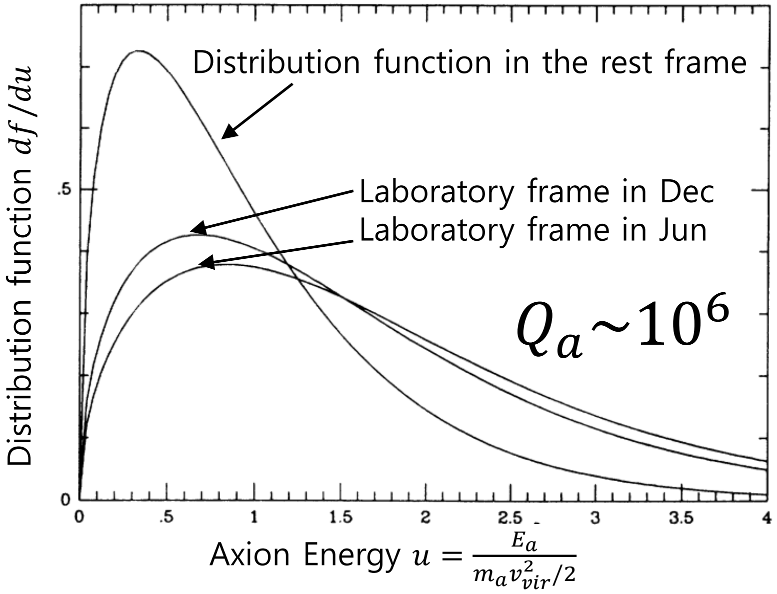

$m_a = 10\ \mu\text{eV}, \quad \rho_{DM} \approx 0.45\ \text{GeV/cm}^3$

$\lambda_a = \frac{2\pi}{m_a v_{vir}} \approx 140\ \text{m},\ N_a = n_a \lambda_a^3 \approx 10^{26},\ \tau_a = \frac{\lambda_a}{v_{vir}} \approx 400\ \mu\text{s}$

Axion

- QCD have non-trivial vacuum structure (θ vacuum). Weinberg, PRD 11 (1975). t'Hooft, PRL 37 (1976).
- The θ vacuum introduces CP violating **'$\boldsymbol{\theta_{QCD}}$ term'** non-perturbatively.

$$S_{\theta_{QCD}} = \int \frac{g^2\theta_{QCD}}{32\pi^2} G^{a\mu\nu}\tilde{G}^{a}_{\mu\nu}\, d^4x \neq 0$$

- **'$\boldsymbol{\theta_{CKM}}$ term'** also can be introduced by chiral rotation with CKM matrix.
- $\theta_{tot} = \theta_{QCD} + \theta_{CKM}$ is physical and can induce neutron EDM.
- The current experimental limit $|\theta_{tot}| < 10^{-10}$ raise naturalness problem.

Abel *et al.*, PRL 124 (2020).

$$\mathrm{d}_n \approx 2.4 \times 10^{-16} |\theta_{tot}|\ \mathrm{e \cdot cm}$$

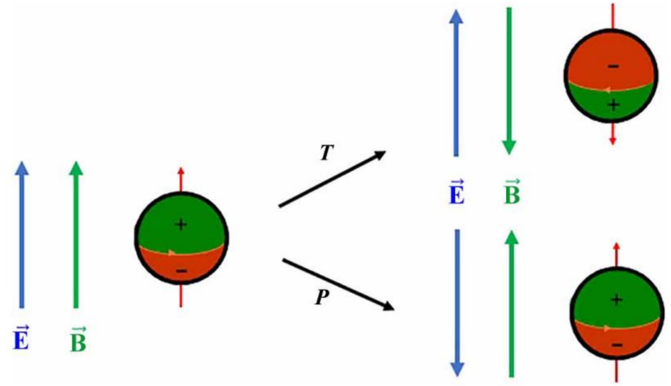

Chadha-Day, Sci. Adv. 8 (2022).

- PQ symmetry breaking of additional scalar particle Φ can dynamically vanish θ term. Peccei & Quinn, PRL 38 (1977), Weinberg, PRL 40 (1978), Wilczek, PRL 40 (1978).
- Axion is a pseudo-Goldstone boson originated from $U(1)_{PQ}$ symmetry breaking.
- The high-mass PQWW axion model was ruled out by accelerator experiments. Edwards *et al.*, PRL 48 (1982). Sivertz *et al.*, PRD 26 (1982). Alam *et al.*, PRD 27 (1983).
- Invisible axion models introduced low-mass axions.
  KSVZ: Kim, PRL 43 (1979). Shifman, Vainshtein, and Zakharov, Nuc. Phys. B, 166 (1980).
  DFSZ: Dine, Fischler, and Srednicki, Phys. Lett. B, 104 (1981). Zhitnitski, Sov. J. Nucl. Phys. 31 (1980).

$$\Phi = \frac{1}{\sqrt{2}}(f_a + \rho)e^{ia/f_a}$$

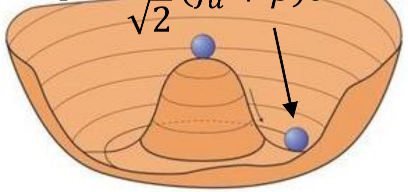

$$\boldsymbol{E \ll \Lambda_{PQ} \sim f_a}$$

$$\mathcal{L}_{CPV} = \frac{g^2}{32\pi^2}\left(\theta_{tot} + \frac{a}{f_a}\right) G^{a\mu\nu}\tilde{G}^a_{\mu\nu}$$

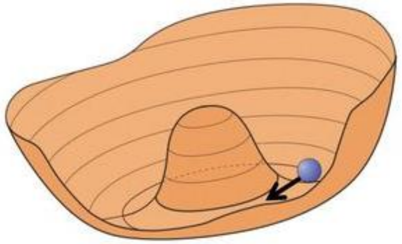

$$\boldsymbol{E \ll \Lambda_{QCD} = 0.3\text{MeV}}$$

$$m_a^2 = \frac{m_u m_d}{(m_u + m_d)^2}\frac{m_\pi^2 f_\pi^2}{f_a^2}$$

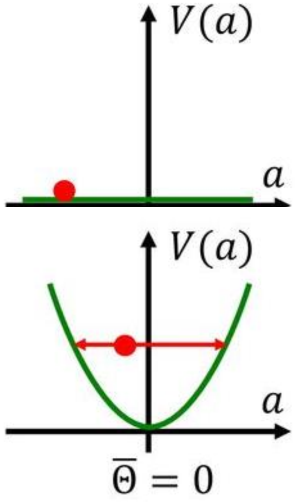

$$\bar{\theta} = \theta_{tot} + \frac{a}{f_a}$$

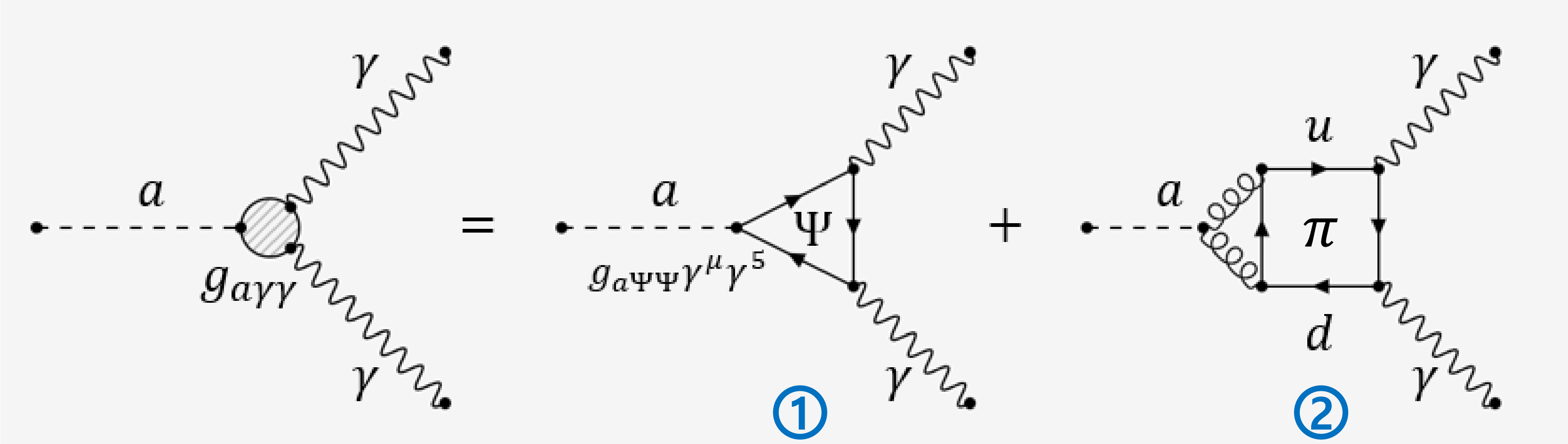

- Invisible axion models
  - Kim-Shiftman-Vainshtein-Zakharov (KSVZ) model
    - ✓ Heavy quark (q) + Yukawa interaction between Φ and Heavy quark
  - Dine-Fisheler-Srednicki-Zhitnitsky (DFSZ) model
    - ✓ PQWW axion + Higher order Yukawa interaction between additional Higgs and SM quarks

PQ charge ① ② Pion mixing

$$g_{a\gamma\gamma} = \frac{\alpha}{\pi f_a}\frac{1}{2}\left[\frac{E}{C} - \frac{2}{3}\frac{4m_d + m_u}{m_d + m_u}\right]$$

$$\frac{E}{C} = 6Q_{q,em}^2 \quad \text{KSVZ}$$

$$\frac{E}{C} = \frac{2}{3}\frac{4X_u + X_d + 3X_e}{X_u + X_d} \quad \text{DFSZ}$$

Cheng *et al.*, PRD 52 (1995).

Introduction:

Axion Dark Matter

- Axion is a cold dark matter candidate.
  Marsh, Phys. Rep. 643 (2016).
  - Axion cosmology suggests the misalignment production mechanism.
  - Small mass invisible axions can be a cold dark matter. Pre-inflationary: $10^{-6} < m_a < 10^{-2}$eV Post-inflationary: 10^{-5} eV $< m_a$
- Axion is considered virialized classical particles in a galactic scale.
  Turner, PRD 42 (1990).
  - Axion follows Maxwell-Boltzmann distribution
- Axion is wave-like in a laboratory scale. $m_a = 10\ \mu\text{eV}$, $\rho_{DM} \approx 0.45\ \text{GeV/cm}^3$

$\lambda_a = \frac{2\pi}{m_a v_{vir}} \approx 140$ m, $N_a = n_a \lambda_a^3 \approx 10^{26}$, $\tau_a = \frac{\lambda_a}{v_{vir}} \approx 400\ \mu s$

Turner, PRD 42 (1990).

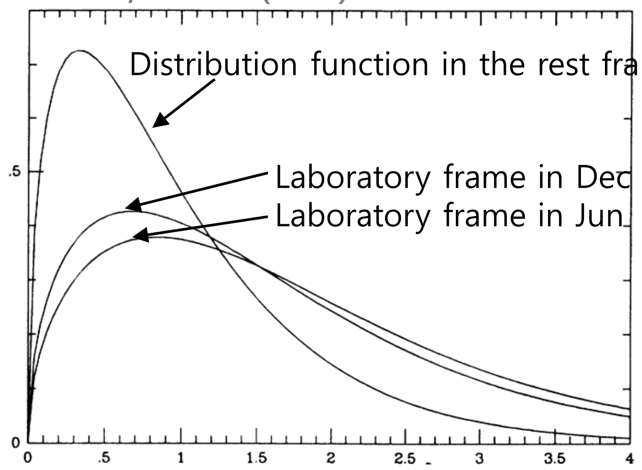

- Axion can emit electromagnetic wave

$$\mathcal{L}_{a-\gamma} = \frac{1}{2}(\partial_\mu a)^2 - \frac{1}{2}m_a^2 a^2 - \frac{1}{4}F_{\mu\nu}F^{\mu\nu} + g_{a\gamma\gamma} a F_{\mu\nu}\tilde{F}^{\mu\nu}$$

$g_{a\gamma\gamma} a \boldsymbol{E} \cdot \boldsymbol{B}$

$$(\partial_t^2 - \nabla^2 + m_a^2)a = -g_{a\gamma\gamma}\mathbf{E}\cdot\mathbf{B}$$
$$\nabla\cdot(\mathbf{E} - c g_{a\gamma\gamma}\mathbf{B}a) = \rho_e/\epsilon$$
$$\nabla\cdot\mathbf{B} = 0$$
$$\nabla\times\mathbf{E} = -\partial_t\mathbf{B}$$
$$\nabla\times(c\mathbf{B} + g_{a\gamma\gamma}\mathbf{E}a) = \partial_t(\mathbf{E} - c g_{a\gamma\gamma}\mathbf{B}a) + c\mu\mathbf{J}_e$$

Coherent Detection?

Introduction:

Cavity Haloscope Experiment for Dark Matter Axion Search

Antenna Coupling (β)

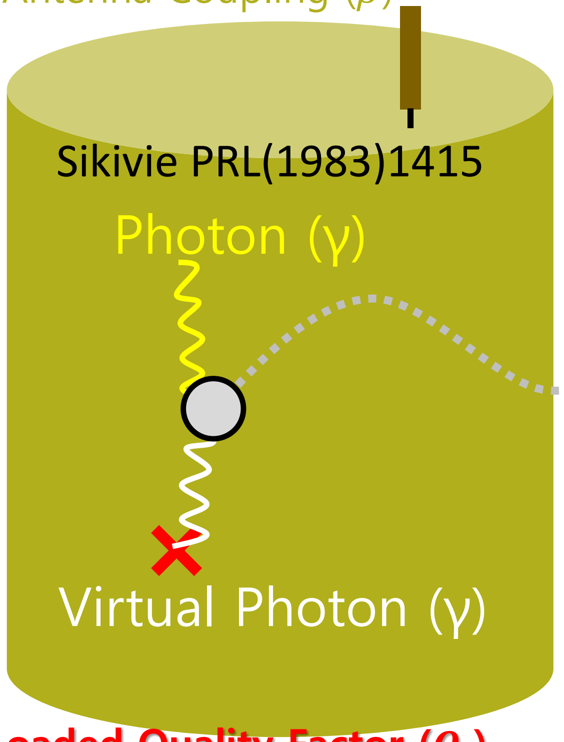

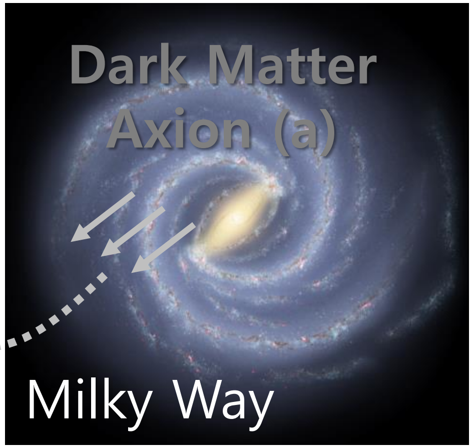

Magnetic Field (B)

Loaded Quality Factor (Q_l)
Volume (V)
Resonant Angular Frequency (ω_0)
Form Factor (C)
System Temperature (T_{sys})

Signal Power

$$P_{sig} = \frac{\beta}{1+\beta} g_{a\gamma\gamma}^2 \frac{\rho_a}{m_a^2} B^2 V \omega_0 C \frac{Q_a Q_l}{Q_a + Q_l}$$

Coupling Constant ($g_{a\gamma\gamma}$); Dark Matter Axion Density (ρ_a); Axion Mass (m_a); Axion Quality Factor (Q_a)

Kim *et al*. JCAP03(2020)066

Scan Rate

$$\frac{df}{dt} \propto \frac{B^4 V^2 C^2}{k_B^2 T_{sys}^2} Q_l Q_a$$

$Q_l \gg Q_a \sim 10^6$

Dr. Jinsu Kim, Patras Workshop, 2023

Introduction:

Cavity Experiment for Coherent Gravitational Wave Detection

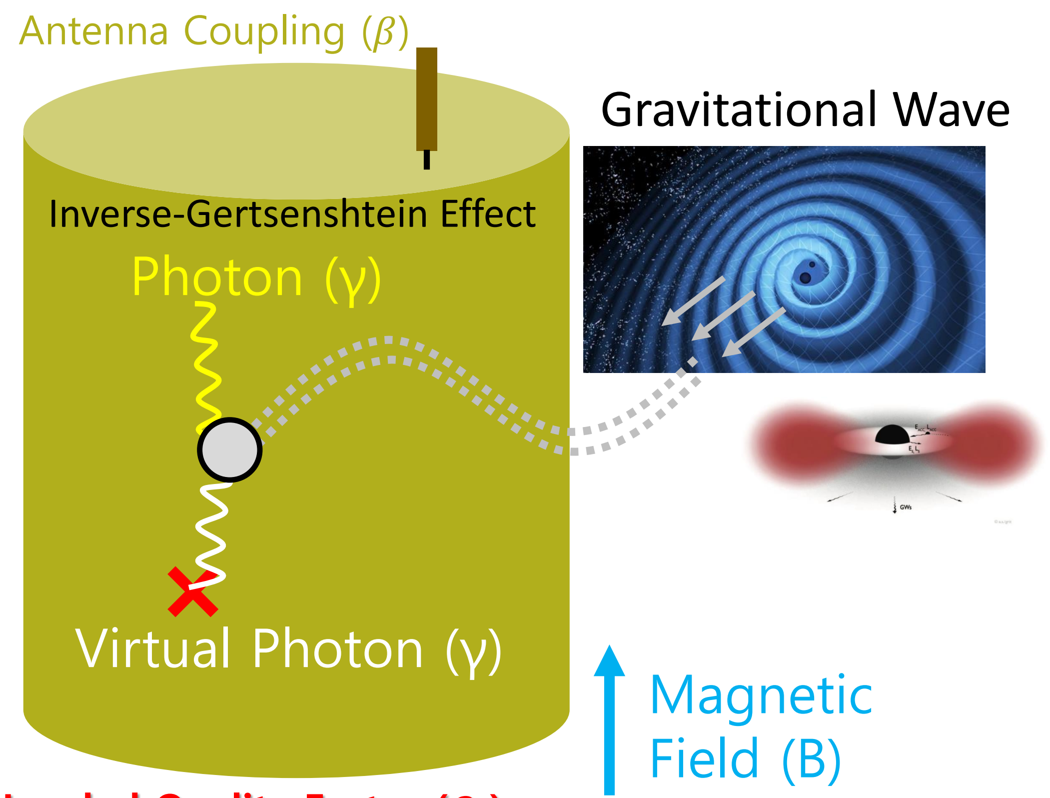

Loaded Quality Factor (Q_l)
Volume (V)
Resonant Angular Frequency (ω_0)
System Temperature (T_{sys})

Signal Power · Coupling Coefficient · Gravitational Wave Strain · Signal Quality Factor

$$P_{sig} = \frac{\beta}{1+\beta}\eta^2 h_g^2 \boldsymbol{B}^2 V^{\frac{5}{3}} \omega_0^3 \frac{Q_g \boldsymbol{Q_l}}{Q_g + \boldsymbol{Q_l}}$$

Berlin *et al*. PRD(2020)105

Scan Rate

$$\frac{df}{dt} \propto \frac{\boldsymbol{B}^4 V^{\frac{10}{3}} \eta^4}{k_B^2 T_{sys}^2} \boldsymbol{Q_l} Q_a$$

$$\boldsymbol{Q_l} \gg Q_g$$

Berlin *et al*. PRD(2020)105

Axion Haloscope Experiment:

Main Axion eXperiment (MAX) at CAPP

- CAPP's flagship experiment to search for axion above 1GHz
- Dine-Fischler-Srednicki-Zhitnitsky (DFSZ) sensitivity

from Andrew Kunwoo Yi's slide

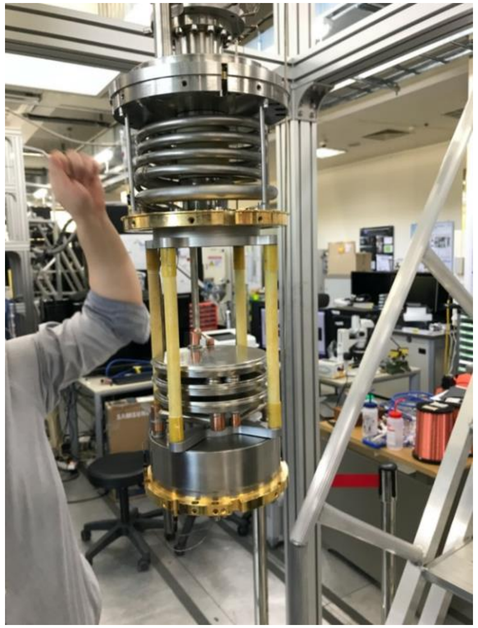

Dilution refrigerator 25mK

+

Josephson Parametric Amplifier

$T_{sys} \approx 200$ mK

+

12 Tesla SC magnet

320mm bore diameter

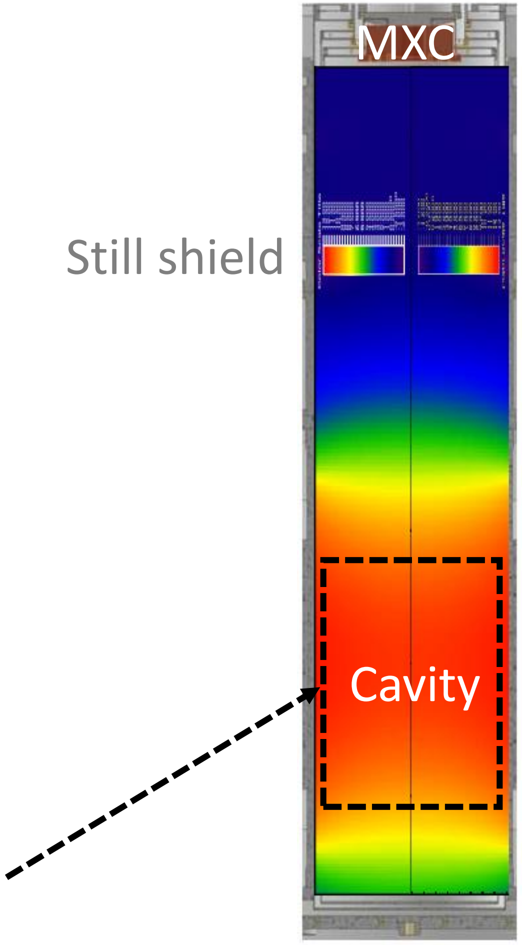

B-field map

Axion Haloscope Experiment:

Analysis Result

arXiv:2402.12892

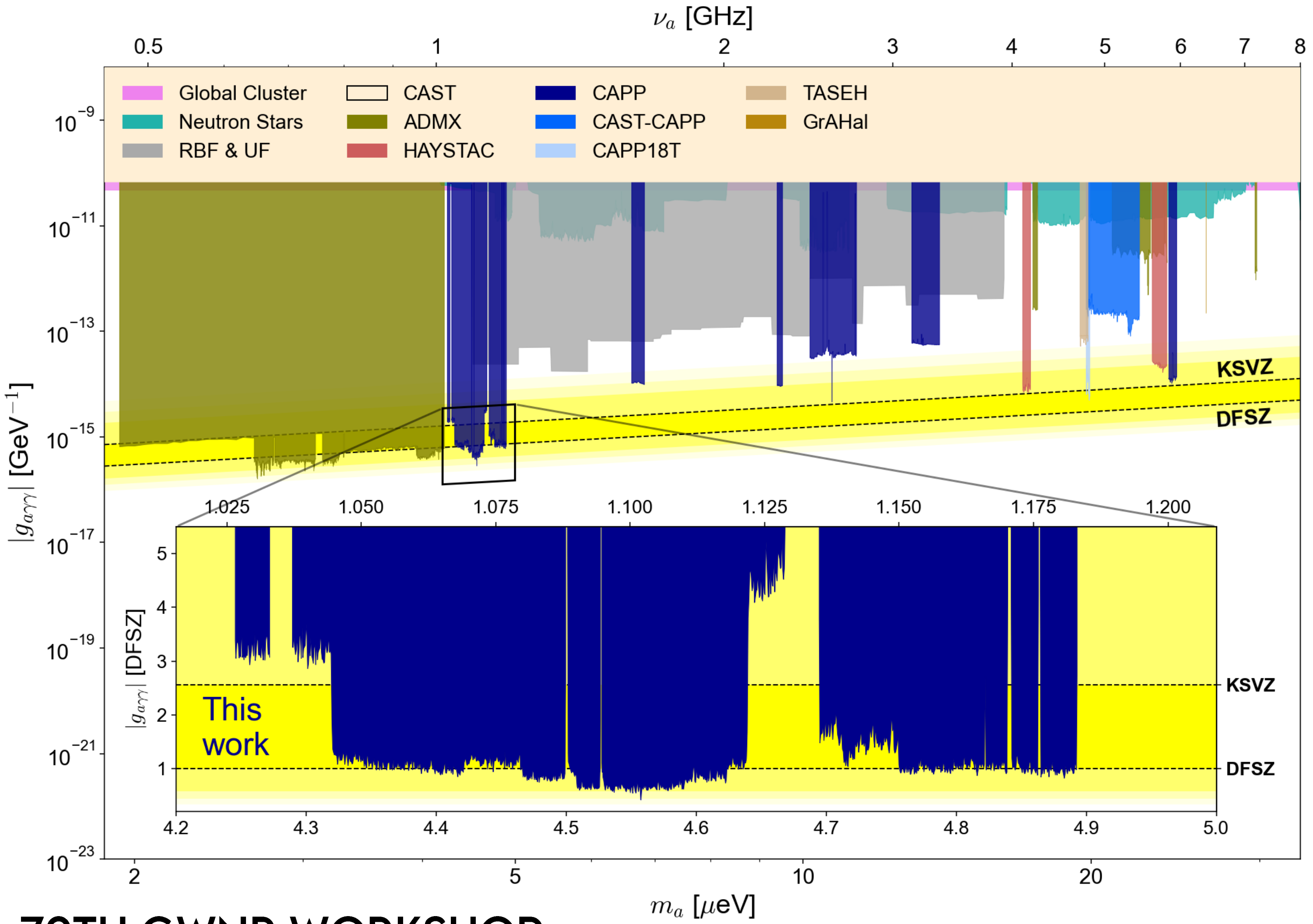

Axion Haloscope Experiment:

Analysis Result

Axion Haloscope Experiment:

Possible Upgrades

- ReBCO have low surface resistance in a high magnetic field.
- Two contributors to low surface resistance.
  - Low vortex number density: **H_{c2} > 100 T (ReBCO)**
  - Vortex pinning is relevant even in a high frequency: **ω_{dp} = 10 - 100 GHz (ReBCO)**

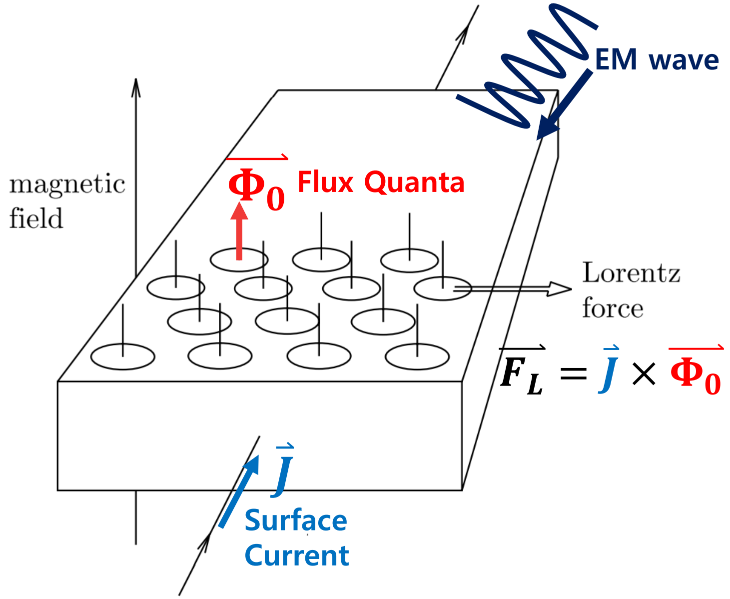

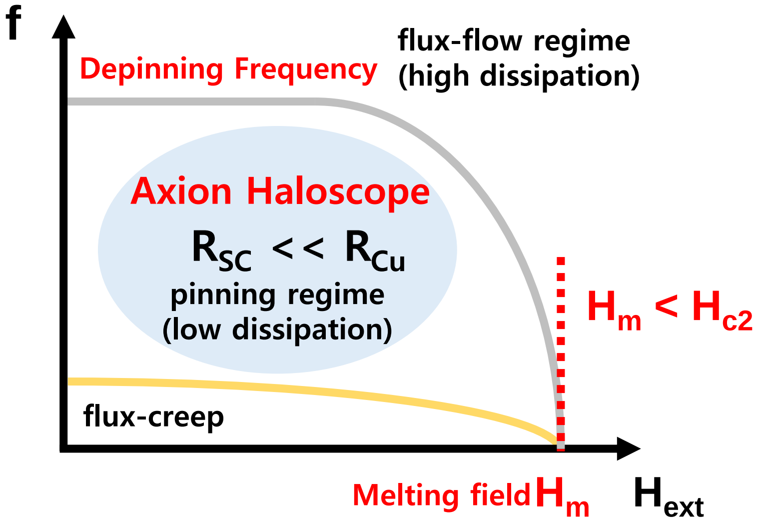

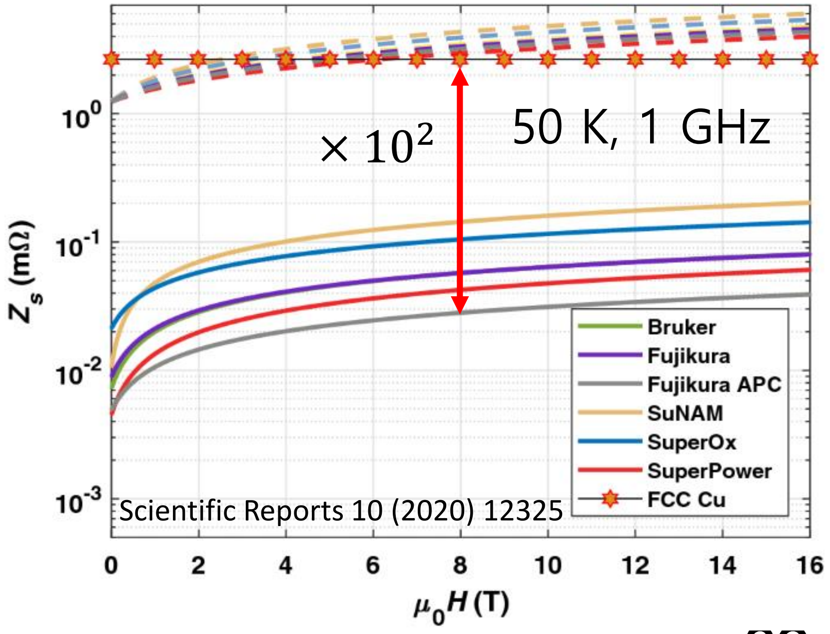

Scientific Reports 10 (2020) 12325

Axion Haloscope Experiment:

Possible Upgrades

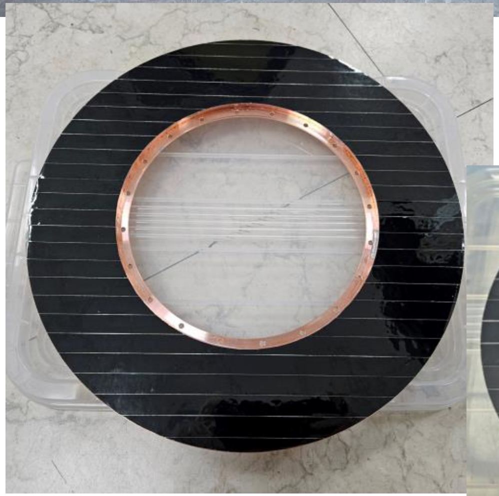

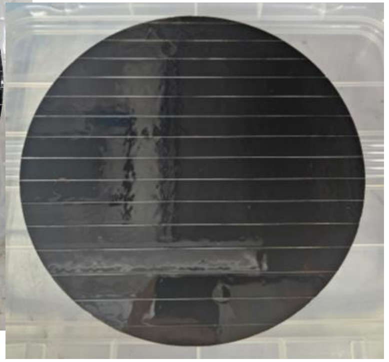

Axion Haloscope Experiment:

Possible Upgrades

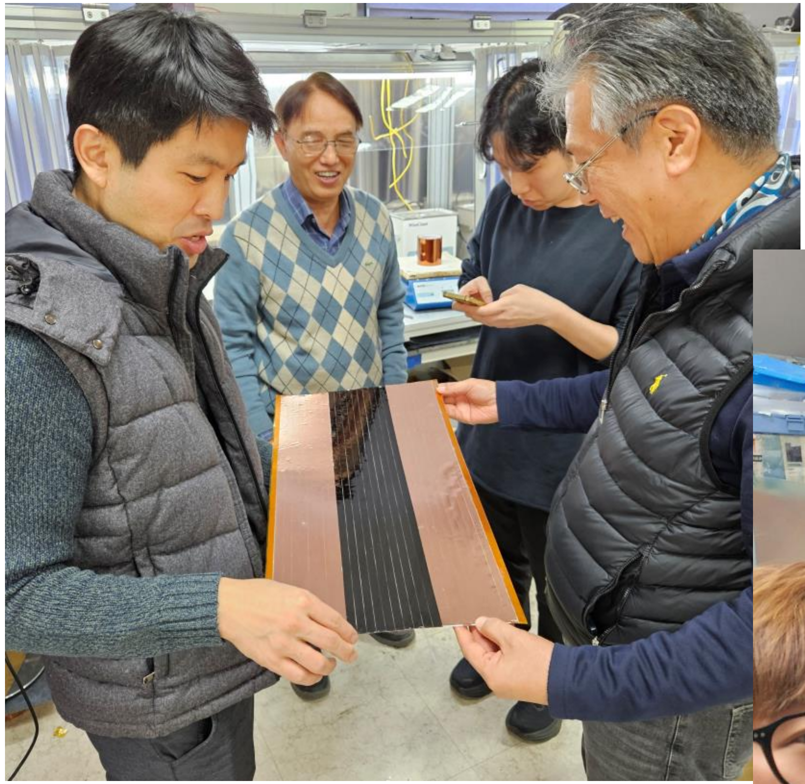

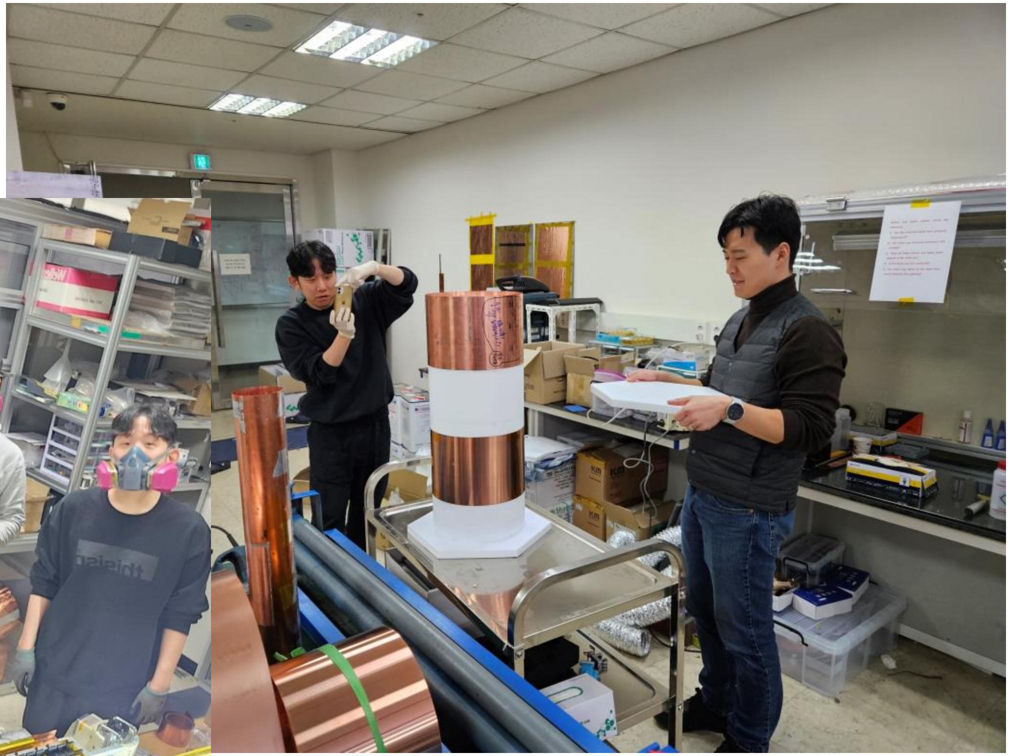

Gravitational Wave Sensitivity of Cavity Experiment:

High Frequency Gravitational Wave Sources - Monochromatic

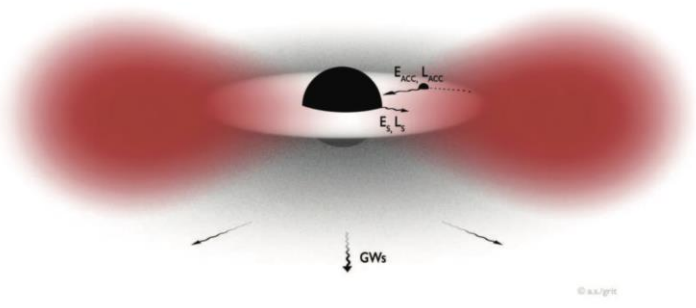

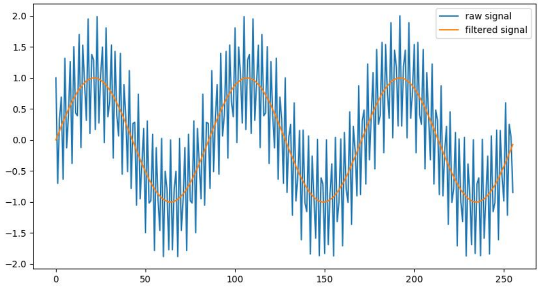

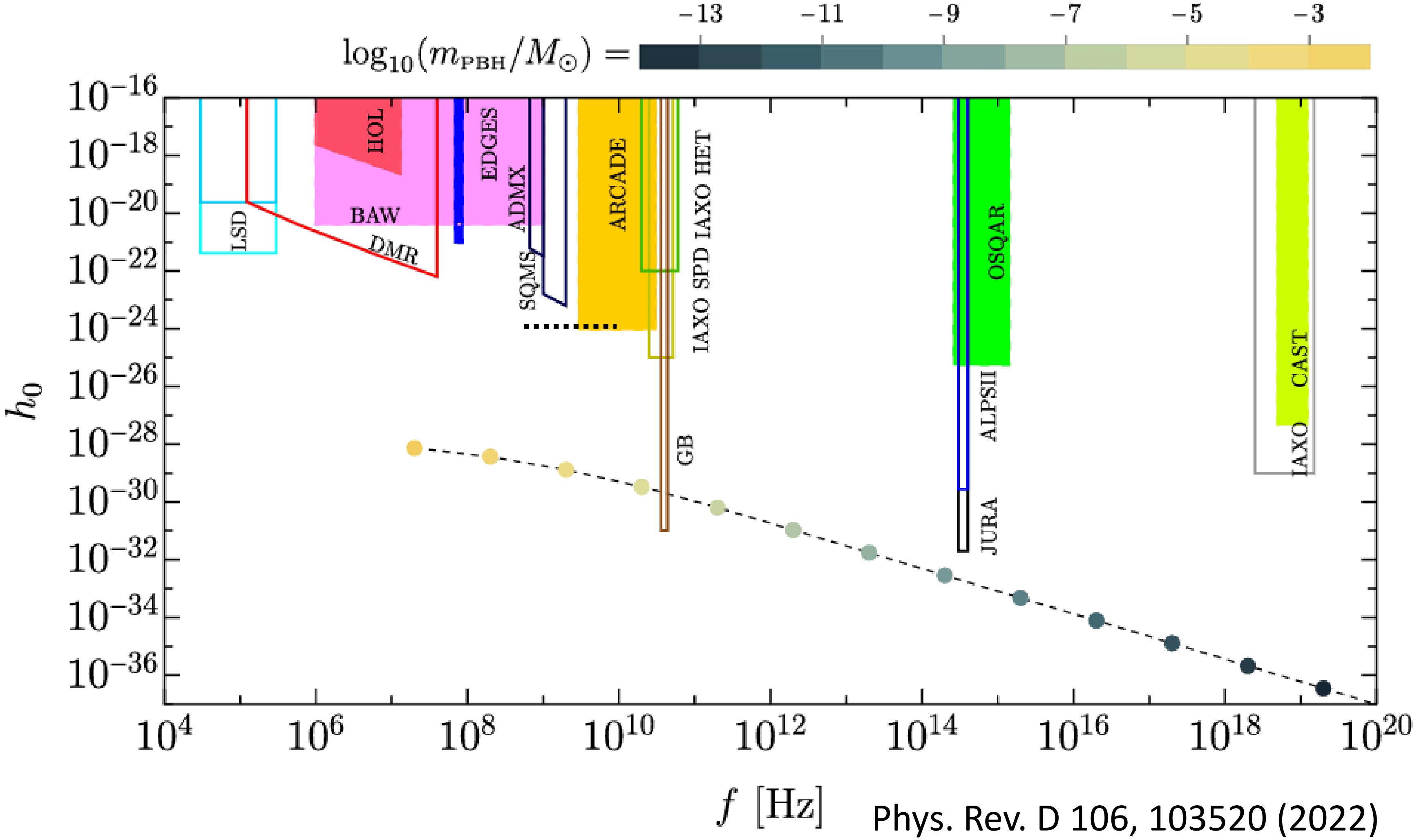

Phys. Rev. D 106, 103520 (2022)

Gravitational Wave Sensitivity of Cavity Experiment:

High Frequency Gravitational Wave Sources - Monochromatic

$$h_0 = 3\times10^{-22}\left(\frac{0.1}{\eta_n}\right)\left(\frac{8\mathrm{T}}{|\mathrm{B}|}\right)\left(\frac{0.1\ \mathrm{m}^3}{V_{\mathrm{cav}}}\right)^{5/6}\left(\frac{10^5}{Q}\right)^{1/2} \times\left(\frac{T_{\mathrm{sys}}}{1\ \mathrm{K}}\right)^{1/2}\left(\frac{1\ \mathrm{GHz}}{f}\right)^{3/2}\left(\frac{\Delta f}{10\ \mathrm{kHz}}\right)^{1/4}\left(\frac{1\ \mathrm{min}}{\Delta t}\right)^{1/4}, \quad (3.11)$$

ADMX:

$Q \approx 8\times10^4, B \approx 7.5\ T$

$V \approx 136\ L, T_{sys} \approx 0.6\ K$

SQMS:

$Q \approx 10^6, B \approx 5\ T$

$V \approx 100\ L, T_{sys} \approx 1\ K$

CAPP:

$Q \approx 10^{6\sim7}, B \approx 12\ T$

$V \approx 36\ L, T_{sys} \approx 0.2\ K$

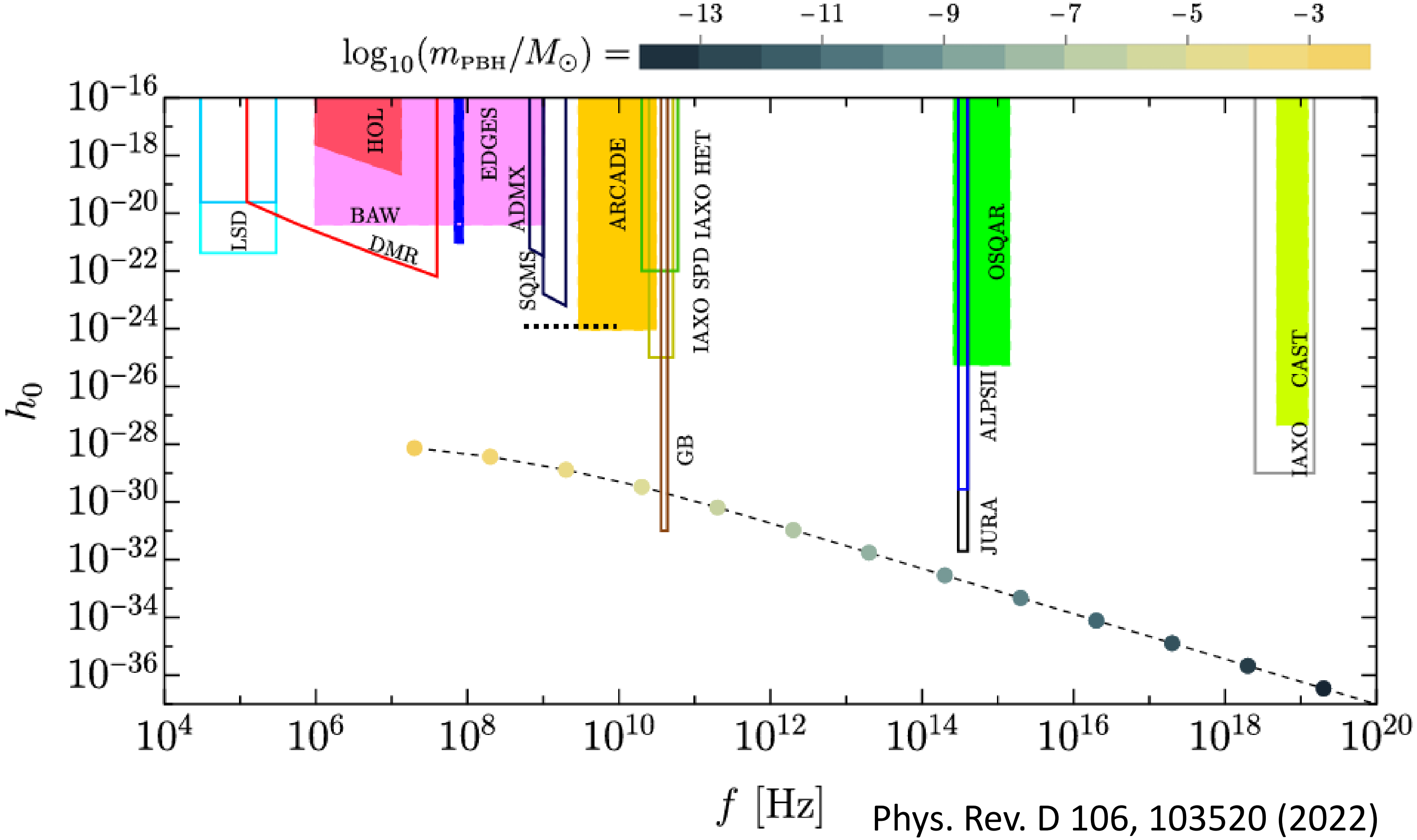

Phys. Rev. D 106, 103520 (2022)

Gravitational Wave Sensitivity of Cavity Experiment:

High Frequency Gravitational Wave Sources - Monochromatic

FermiLab MAGO 2.0

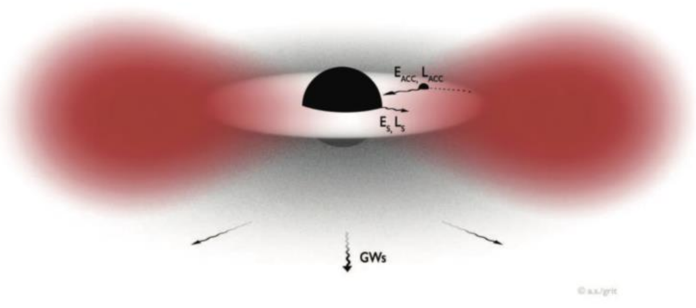

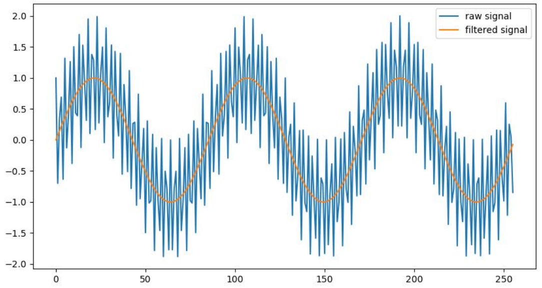

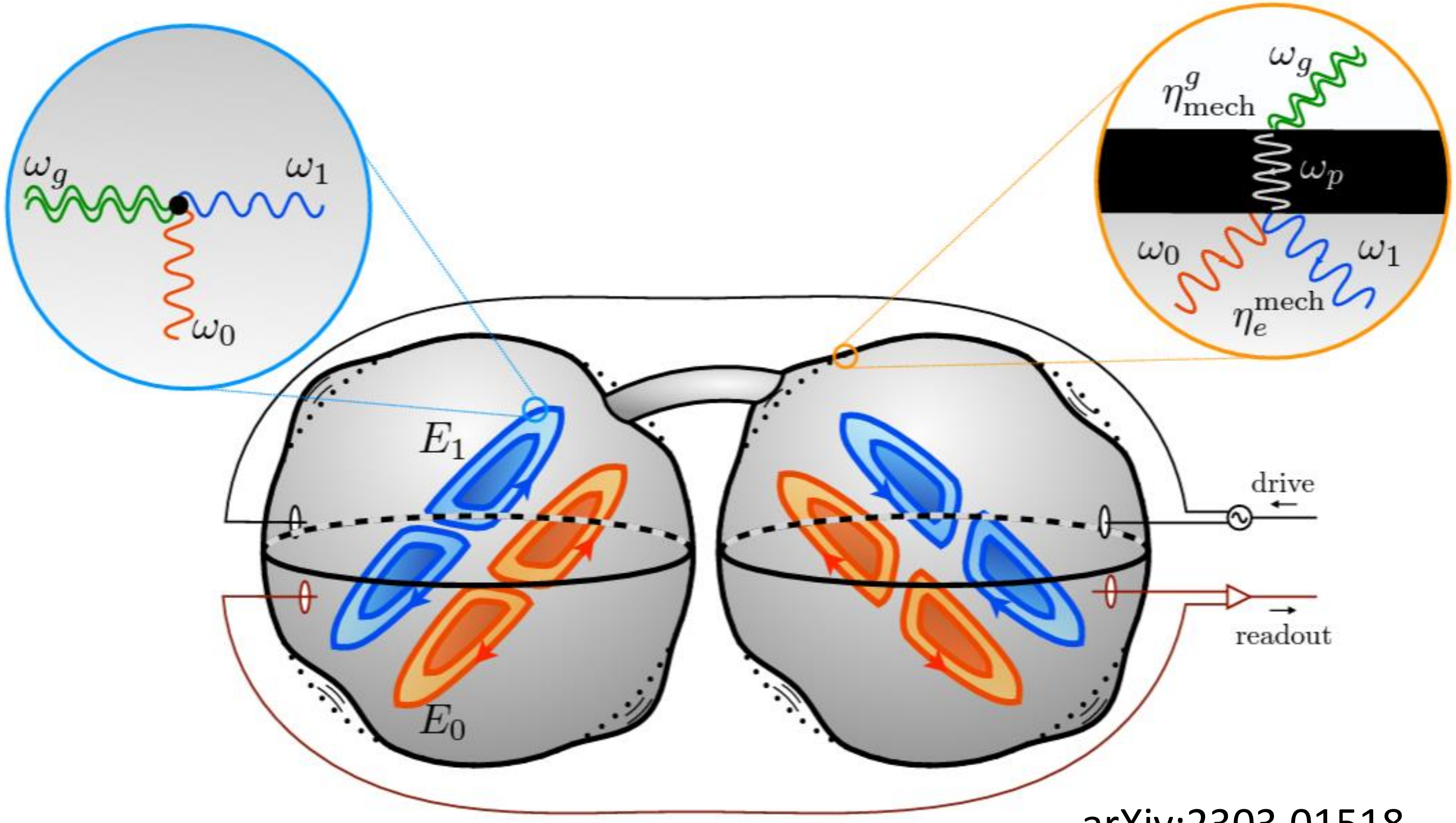

arXiv:2303.01518

Gravitational Wave Sensitivity of Cavity Experiment:

High Frequency Gravitational Wave Sources - Monochromatic

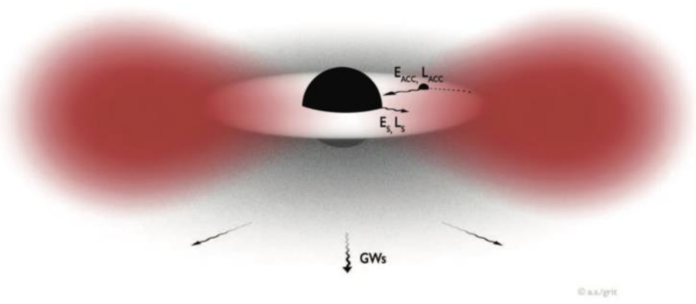

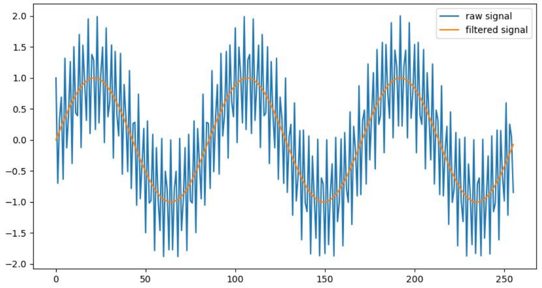

FermiLab MAGO 2.0

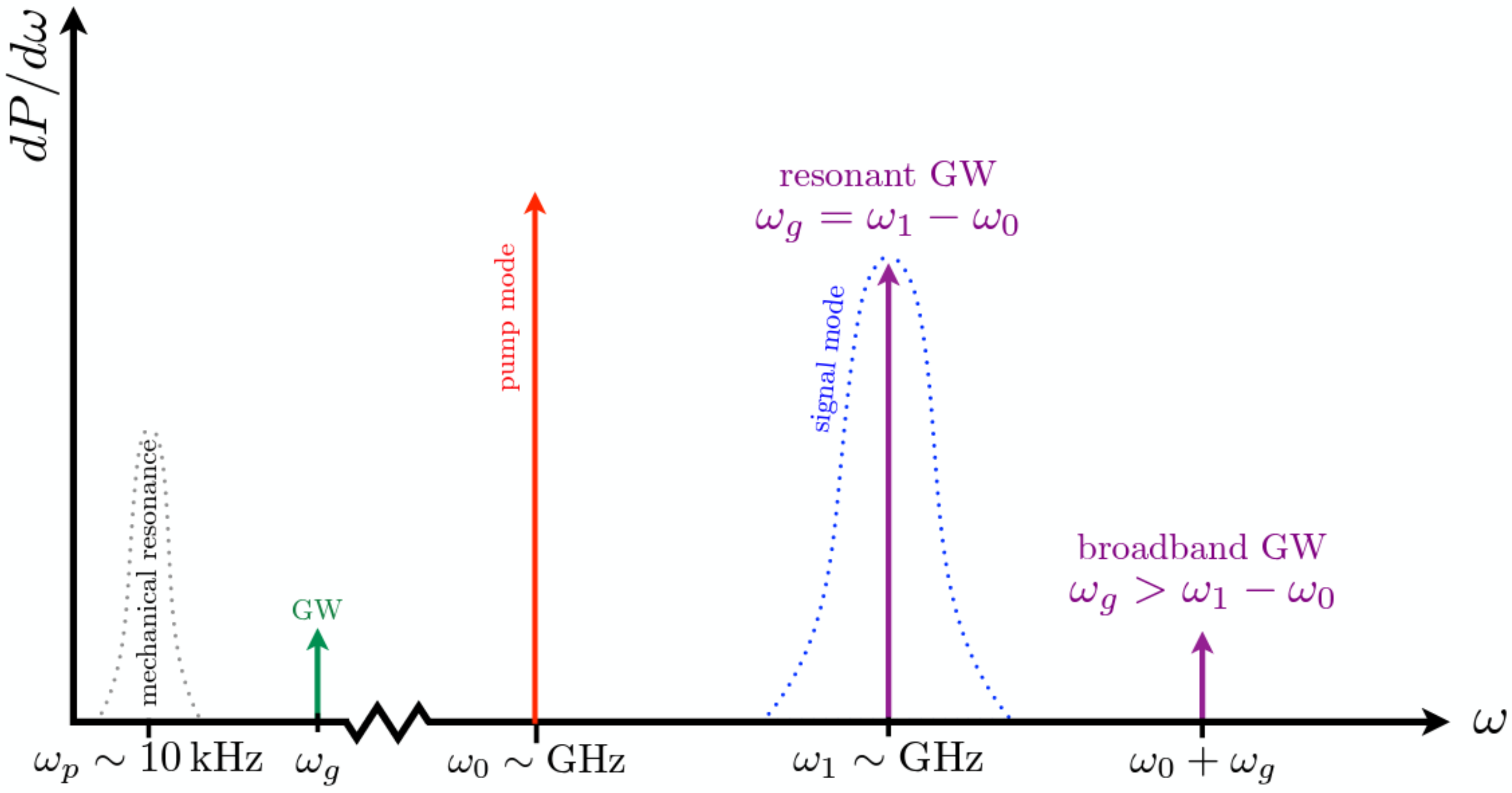

arXiv:2303.01518

Gravitational Wave Sensitivity of Cavity Experiment:

High Frequency Gravitational Wave Sources - Monochromatic

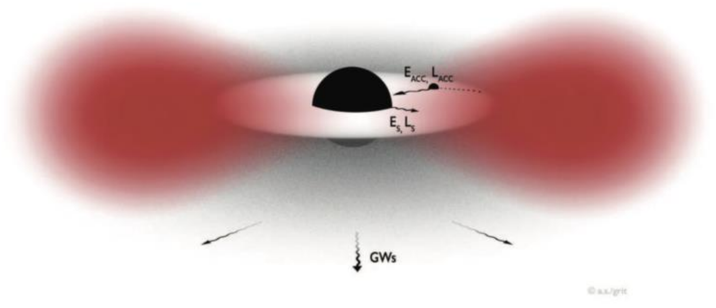

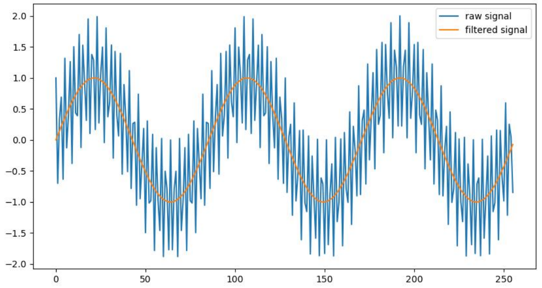

FermiLab MAGO 2.0

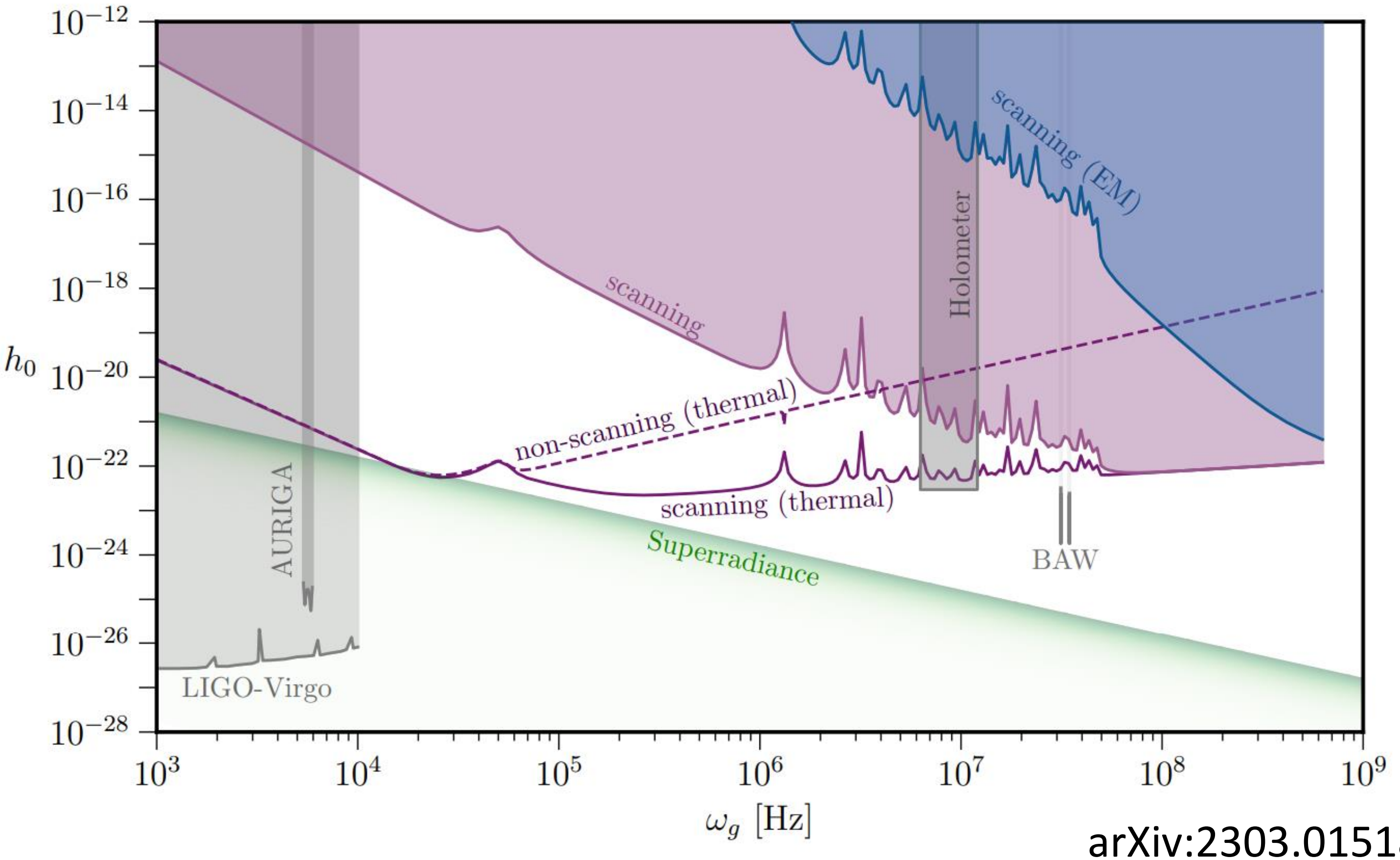

arXiv:2303.01518

Gravitational Wave Sensitivity of Cavity Experiment:

High Frequency Gravitational Wave Sources - Transient

Miller, M.C., Yunes, N. Nature 568, 469–476 (2019).

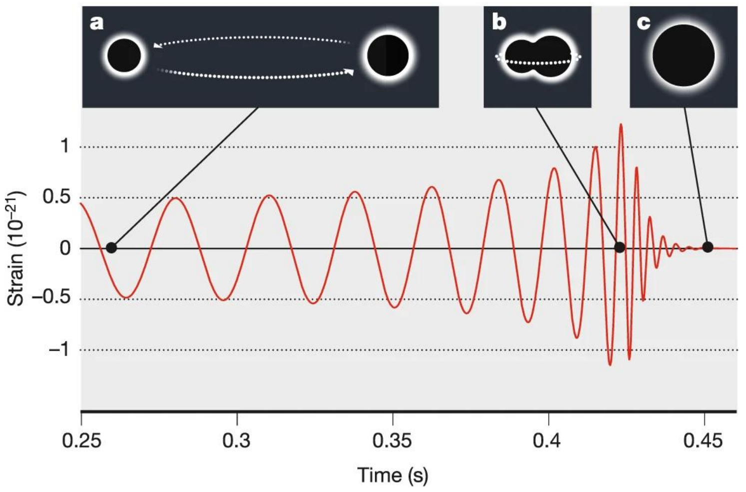

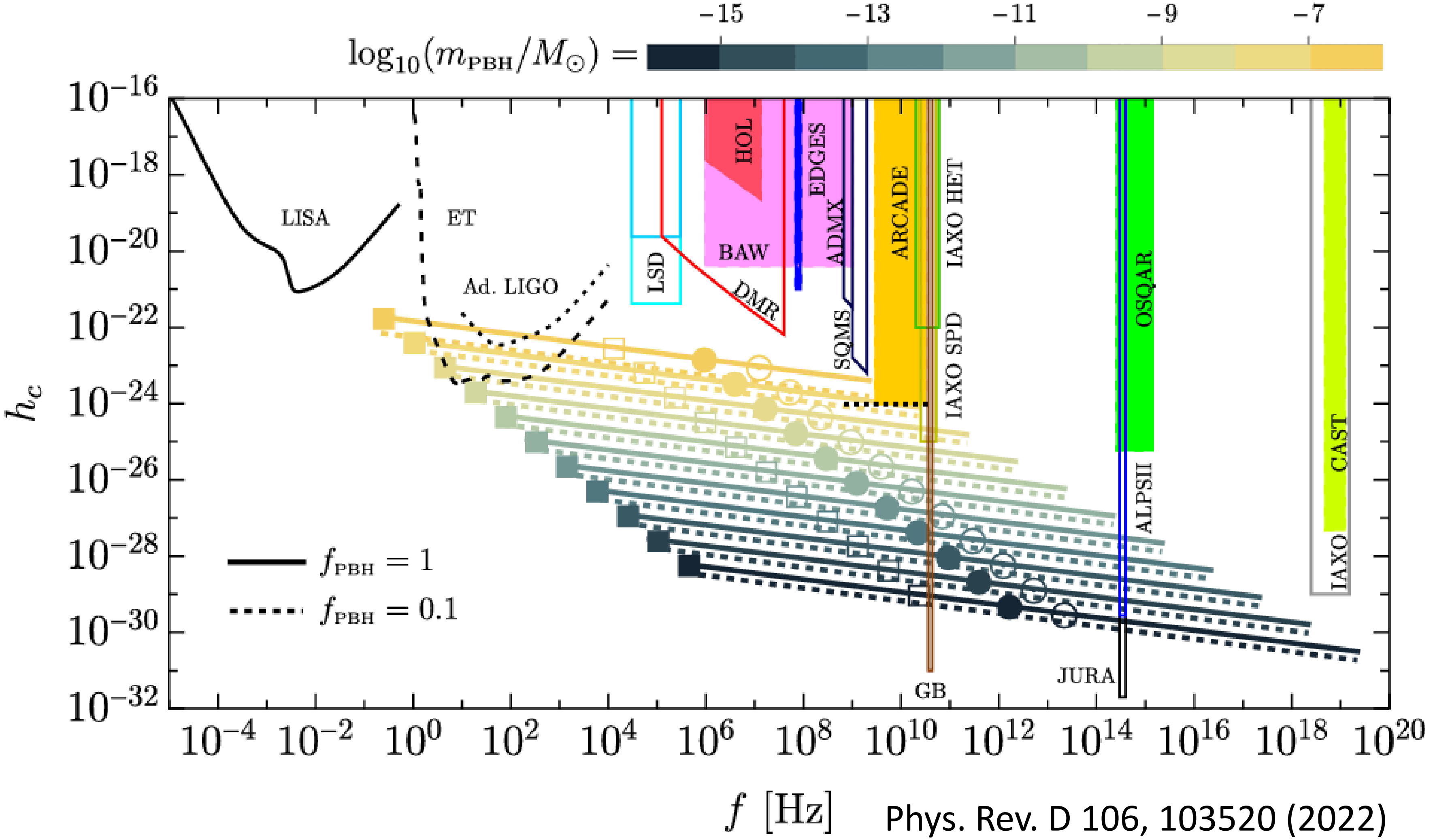

Phys. Rev. D 106, 103520 (2022)

Gravitational Wave Sensitivity of Cavity Experiment:

High Frequency Gravitational Wave Sources - Transient

Miller, M.C., Yunes, N. Nature 568, 469–476 (2019).

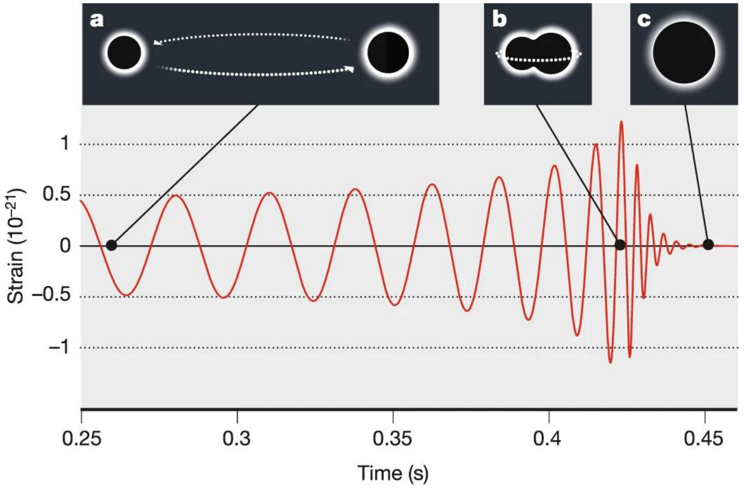

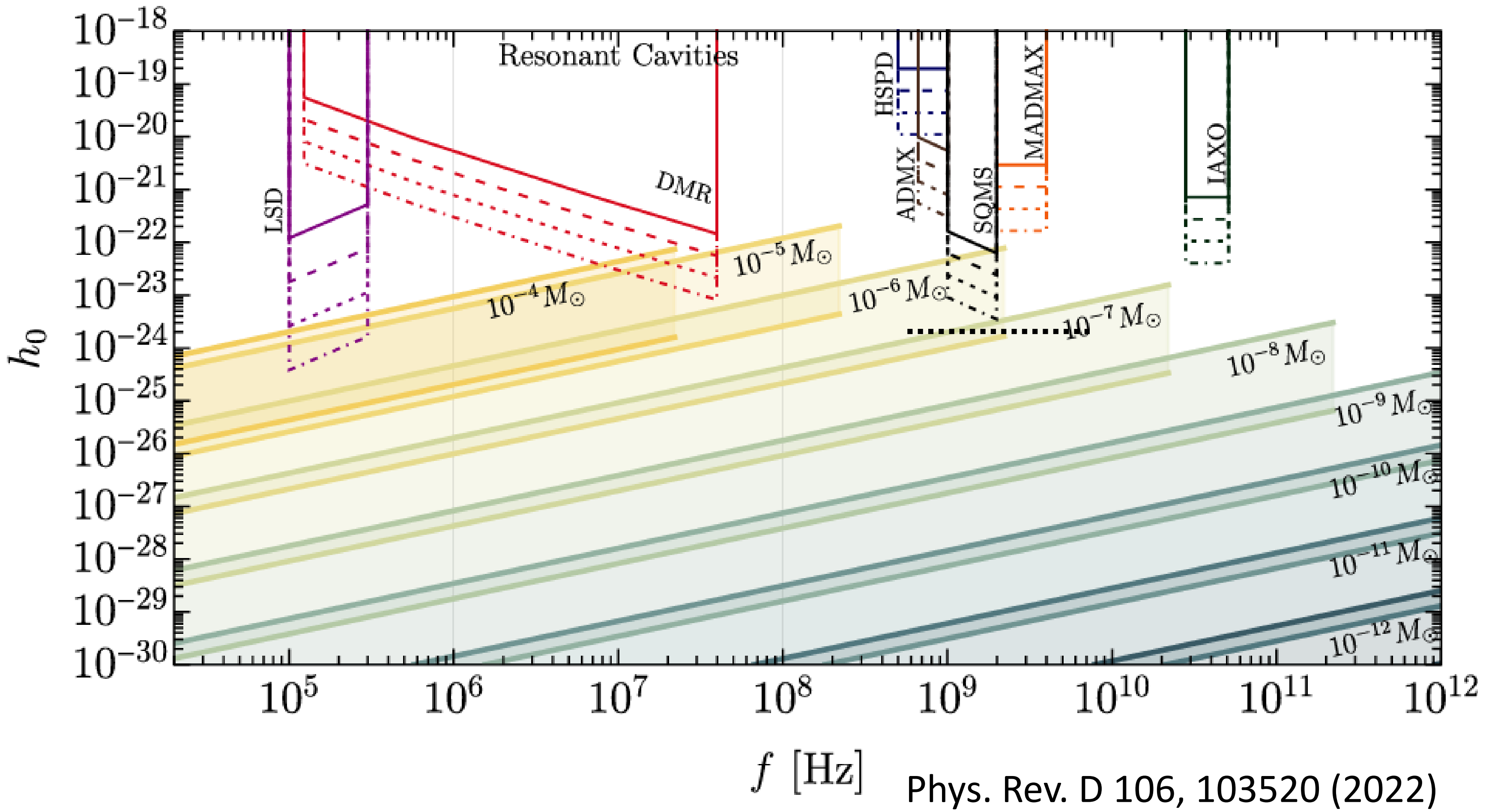

Phys. Rev. D 106, 103520 (2022)

Gravitational Wave Sensitivity of Cavity Experiment:

High Frequency Gravitational Wave Sources - Transient

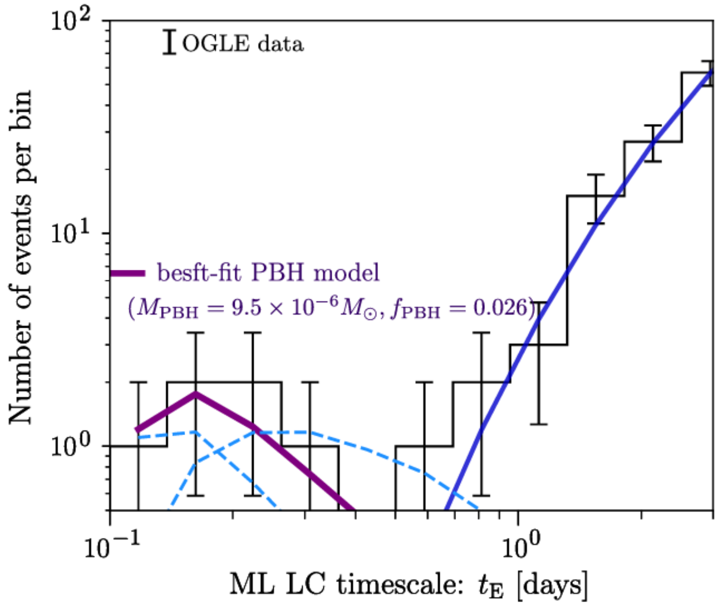

Phys. Rev. D 99, 083503

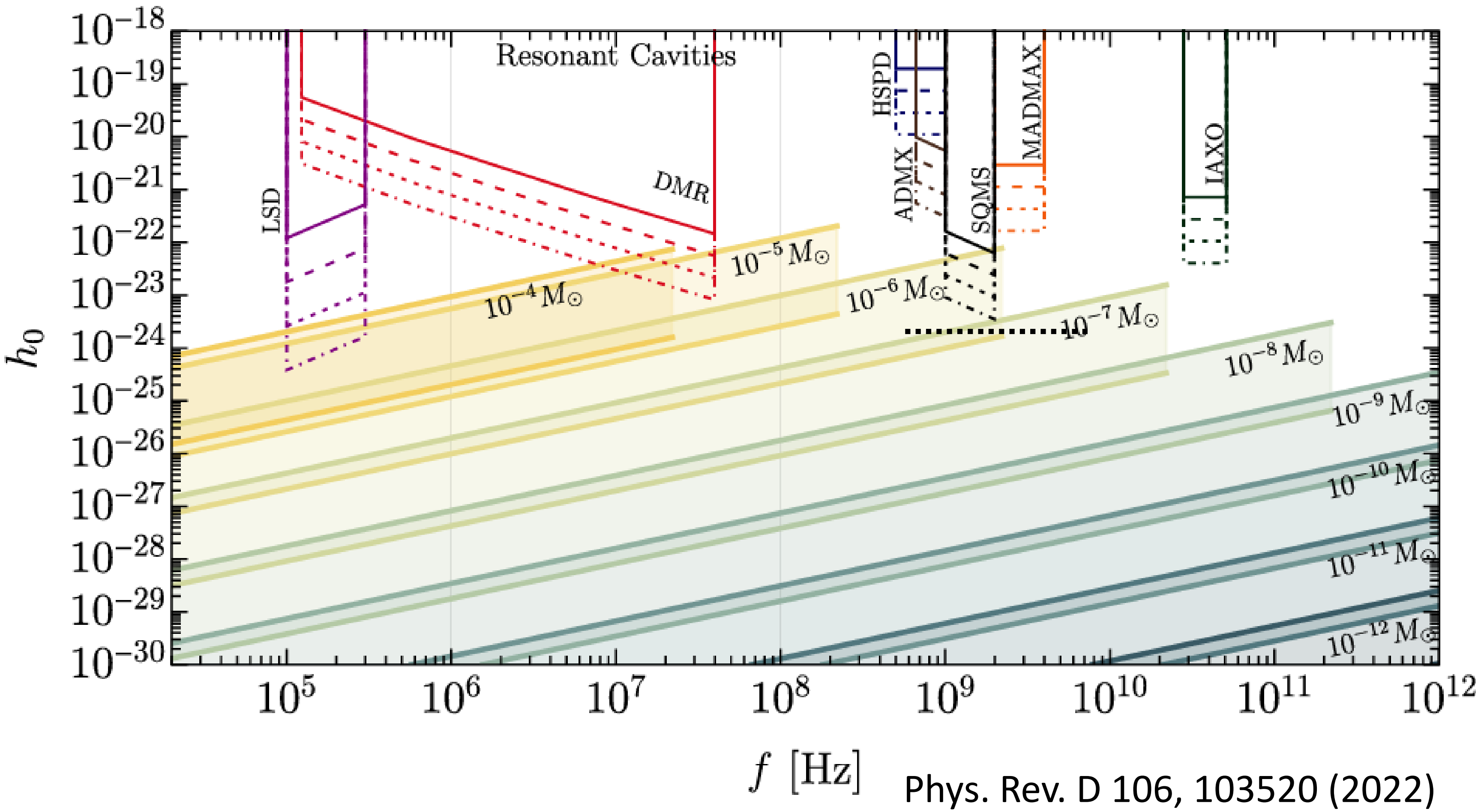

Phys. Rev. D 106, 103520 (2022)

Gravitational Wave Sensitivity of Cavity Experiment:

High Frequency Gravitational Wave Sources - Stochastic

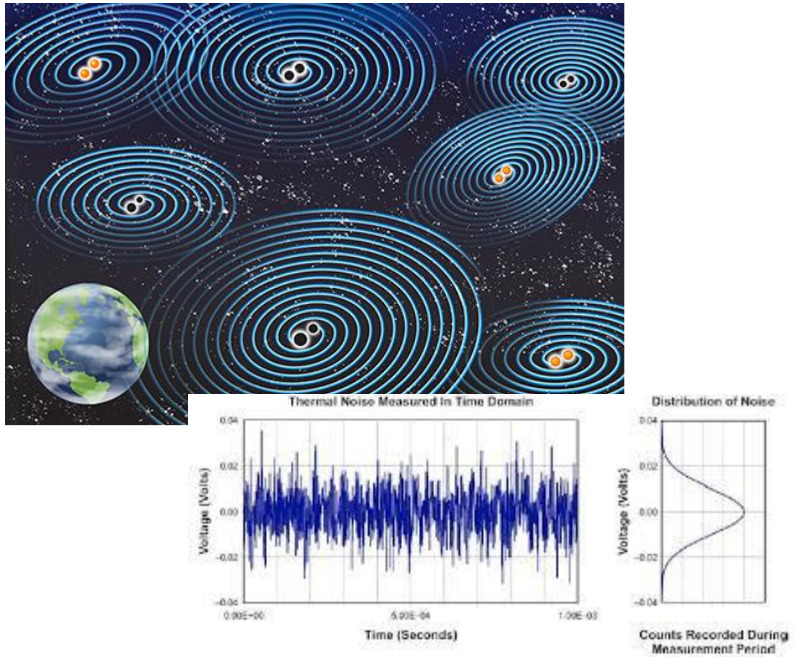

https://physics.aps.org/articles/v13/113

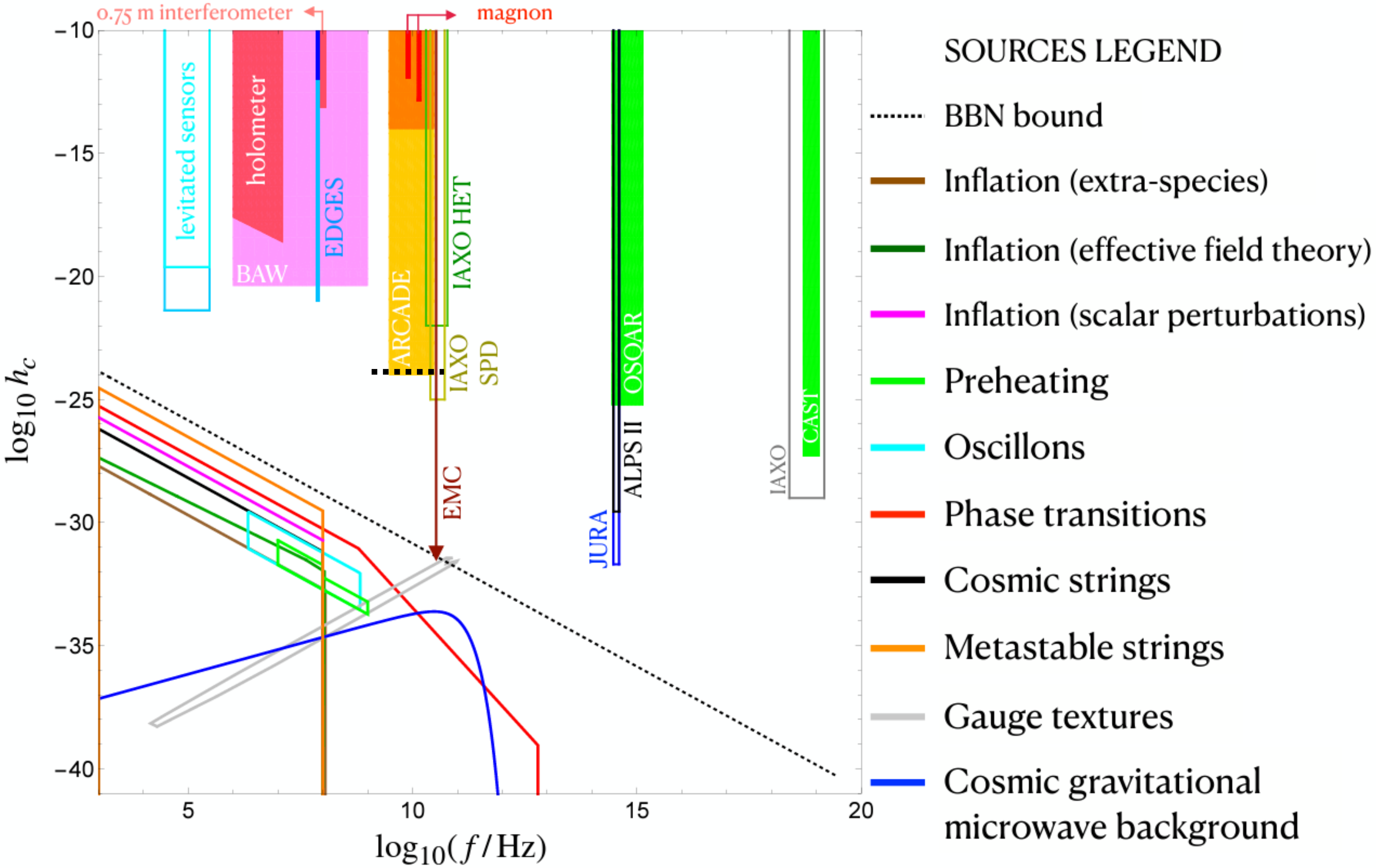

Living. Rev. Relativ. 24, 4 (2021).

Gravitational Wave Sensitivity of Cavity Experiment:

High Frequency Gravitational Wave Sources - Stochastic

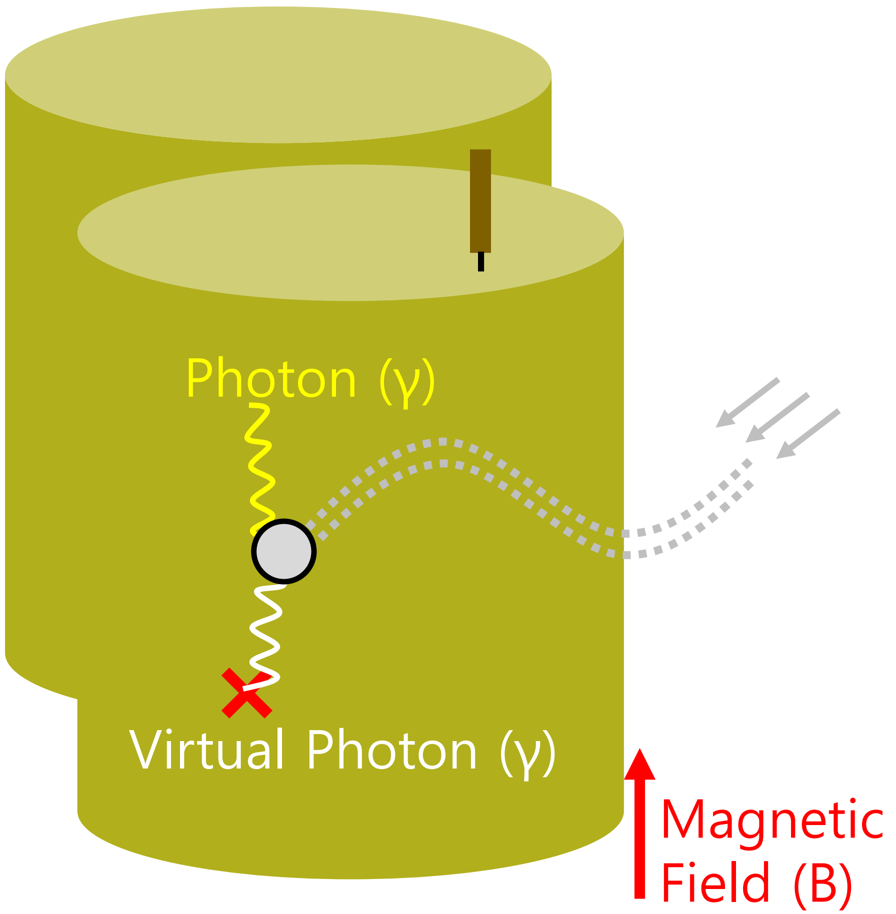

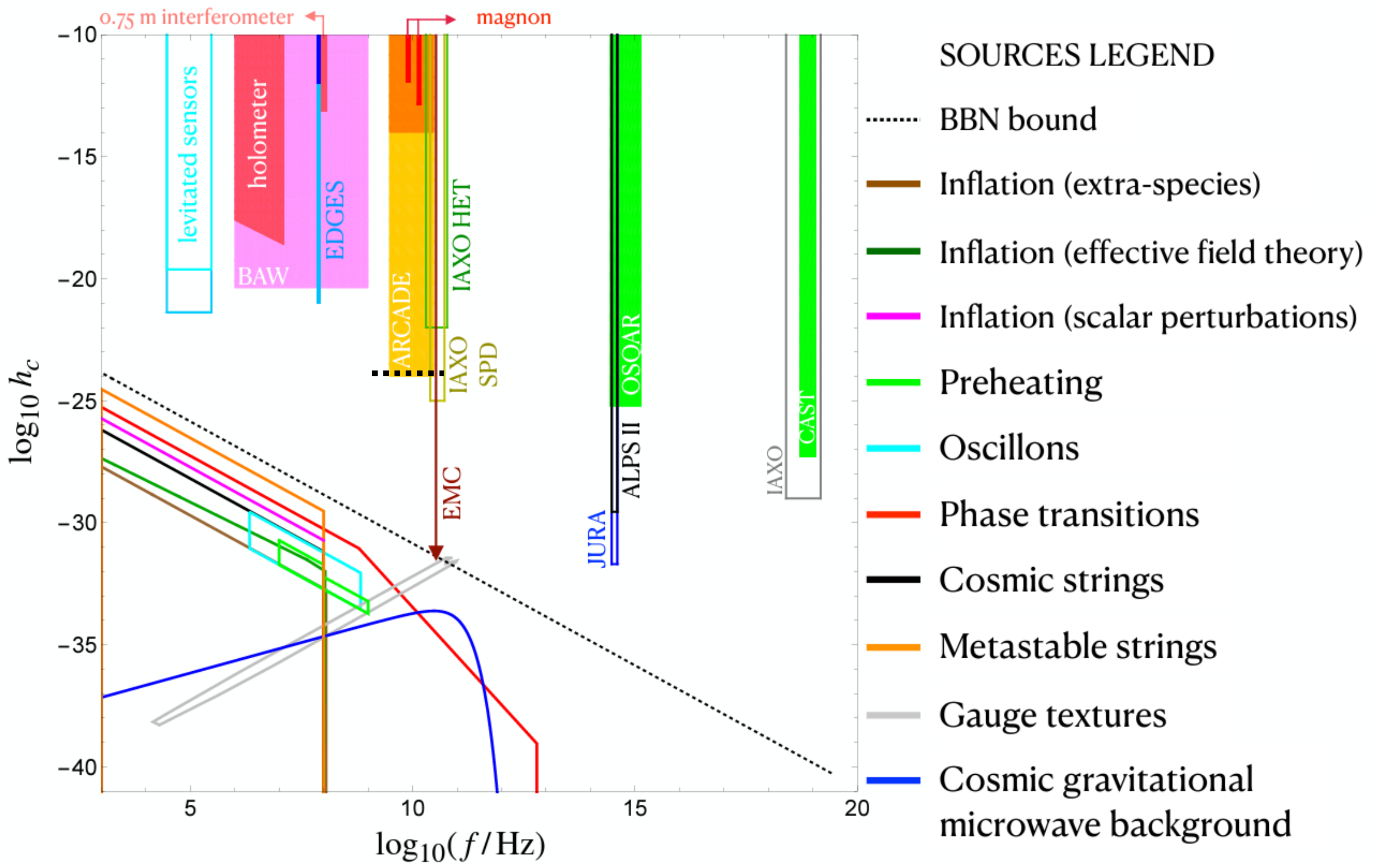

Living. Rev. Relativ. 24, 4 (2021).

Gravitational Wave Sensitivity of Cavity Experiment:

High Frequency Gravitational Wave Sources - Stochastic

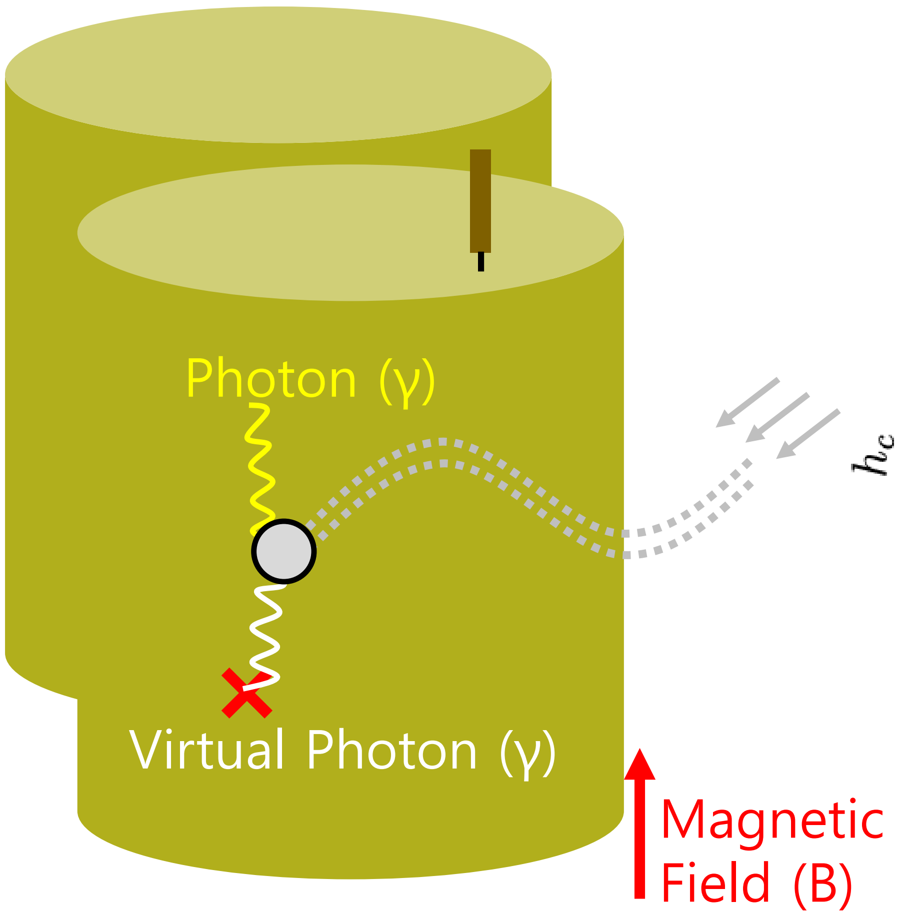

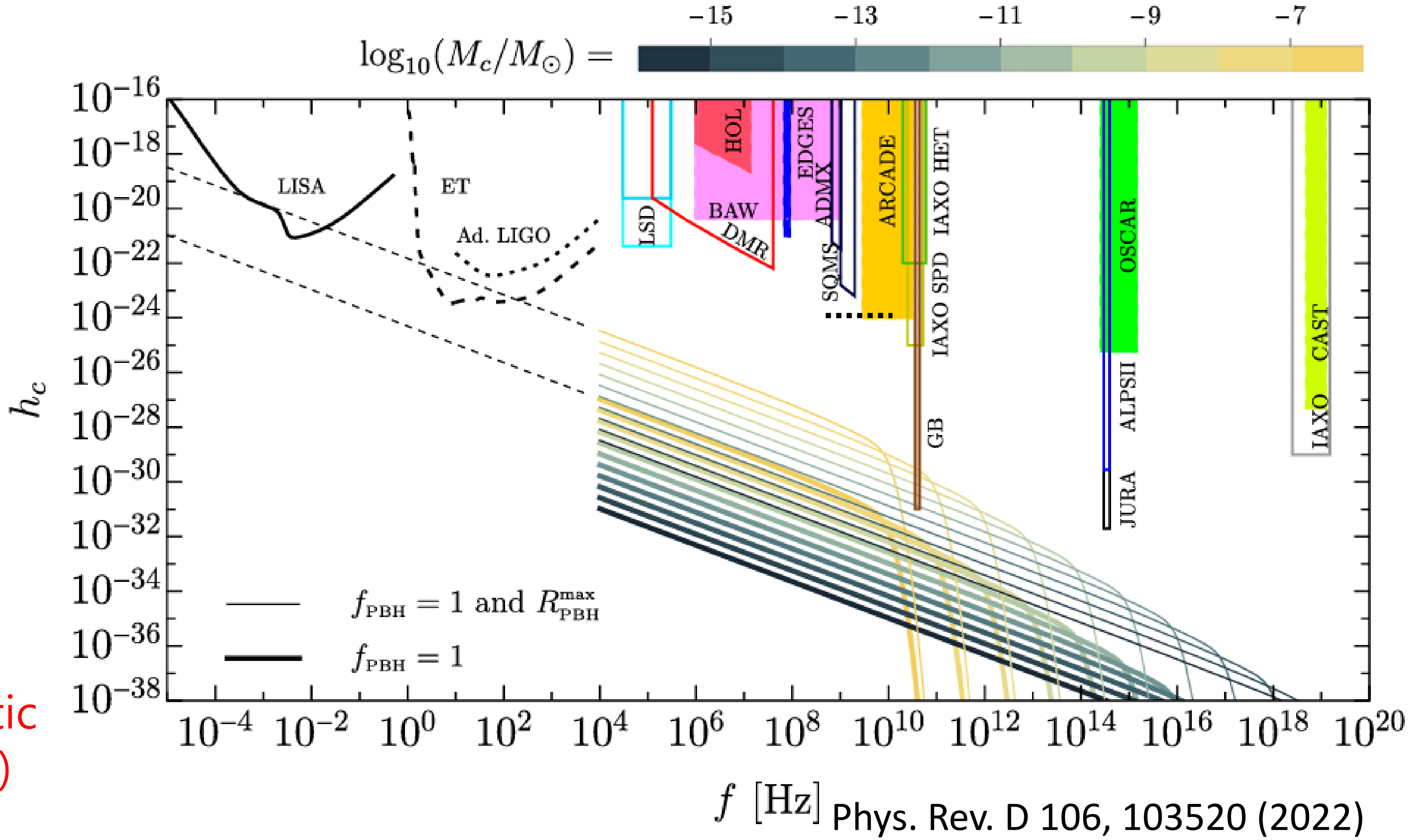

Phys. Rev. D 106, 103520 (2022)

Gravitational Wave Sensitivity of Cavity Experiment:

High Frequency Gravitational Wave Sources - Stochastic

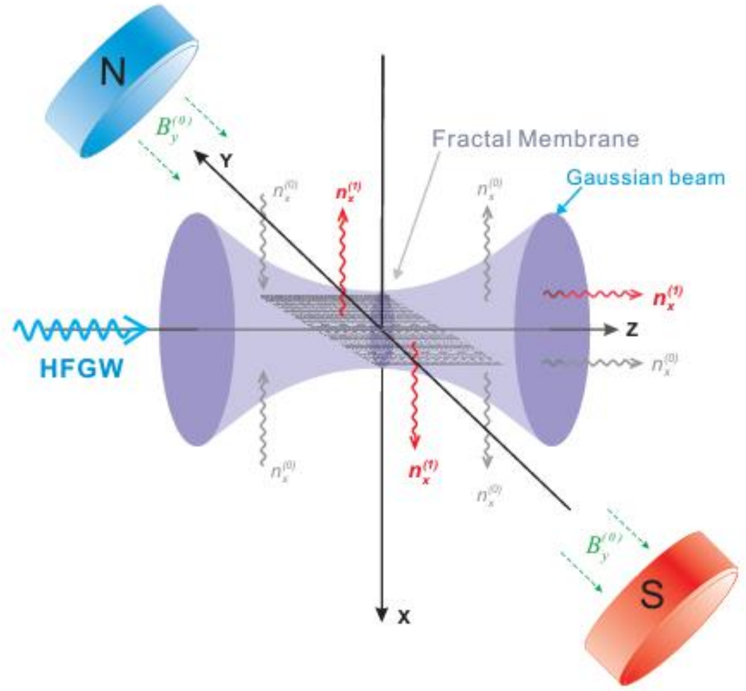

Int. J. Theor. Phys. 55, 3506–3514 (2016)

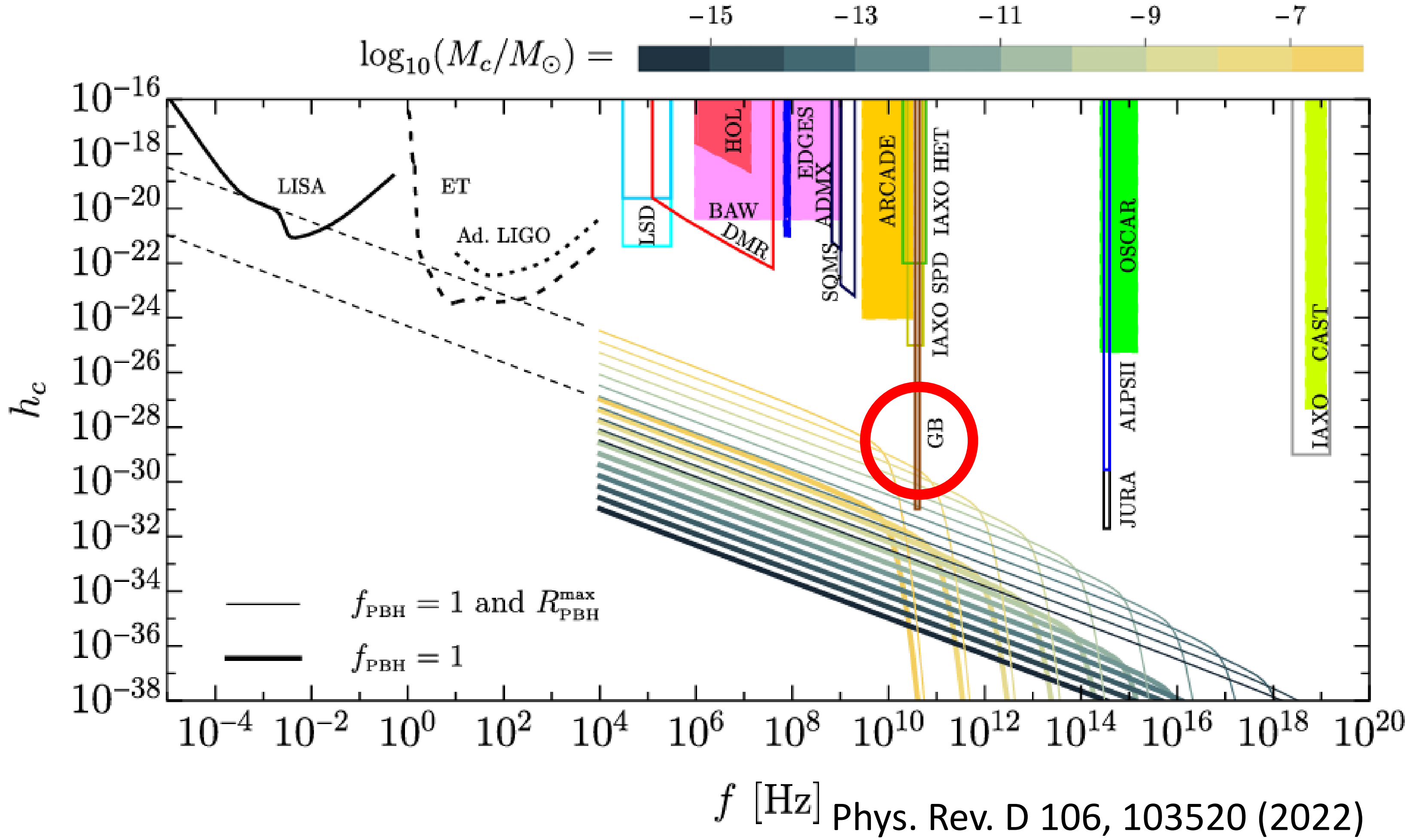

Phys. Rev. D 106, 103520 (2022)

Introduction:

High Frequency Gravitational Wave Sources - Stochastic

- High-frequency gravitational wave (GW) search will open the new window for astrophysics and cosmology.
- Cavity haloscope for dark matter axion search also can detect signals from the interaction between electromagnetic (EM) resonant mode and high-frequency gravitational wave.
- Cavity experiment have enough sensitivity to target transient signal from primordial blackhole binaries which supported by Optical Gravitational Lensing Experiment (OGLE).
- Understanding the background physics under EM-GW interaction and new data analysis method is required.
- Stochastic gravitational wave detection needs new experimental concept.